

Factors affecting temporal variation in occupancy of two common species of
butterflies in woodlands of the eastern United States, *Papilio*
glaucus and *Eurytides marcellus*.

Angela Louise Zappalla

Herndon, Virginia

B.S. Wildlife Conservation, University of Delaware, 2013

A Thesis presented to the Graduate Faculty
of the College of William and Mary in Candidacy for the Degree of
Master of Science

Department of Biology

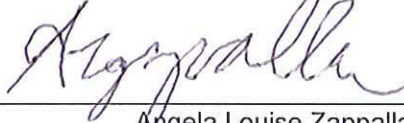
The College of William and Mary

May 2016

APPROVAL PAGE

This Thesis is submitted in partial fulfillment of
the requirements for the degree of

Master of Science



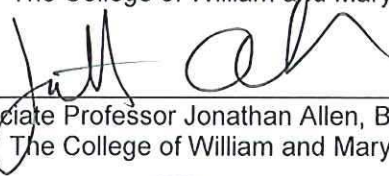
Angela Louise Zappalla

Approved by the Committee, April 2016

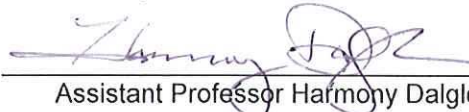


Committee Chair

Associate Professor Matthias Leu, Biology
The College of William and Mary



Associate Professor Jonathan Allen, Biology
The College of William and Mary



Assistant Professor Harmony Dagleish, Biology
The College of William and Mary



Dr. Erica Fleishman
University of California, Davis

ABSTRACT PAGE

Identifying key factors of habitat quality and the extents at which they operate is invaluable to the understanding of the biology of a species. Key factors defining habitat quality for many common butterfly species have yet to be determined. Diverse methods are used to define habitat quality for butterflies. Some of these, such as mark-release-recapture or distance sampling, can be difficult to implement. Occupancy modeling is less invasive and generally less expensive than these other methods. Occupancy modeling is based on repeated presence-absence surveys. Occupancy is the probability that a species is present at a given site after accounting for imperfect detection. Detection is the probability that a species is detected given that it is present. The goal of this study was to identify factors at different spatial extents that are associated with occupancy, colonization (the probability that a site that was unoccupied in the previous time step is occupied in the current time step), and extinction (the probability that a site that was occupied in the previous time step is vacant in the current time step) of two common butterfly species in woodlands of the eastern United States, *Eurytides marcellus* and *Papilio glaucus*. For both species, the count and or proportion of host plants explained the greatest variation in occupancy. For *E. marcellus*, the greatest proportion of variation in probabilities of colonization and extinction was explained by the proportion of agricultural cover and the density of edges between forests and open-herbaceous areas and between forests and wetlands. The variables with which occupancy, colonization, and extinction of *E. marcellus* were most strongly associated were measured at extents from 90 m-5 km. Variables that explained the greatest variation in occupancy, colonization, and extinction of *P. glaucus* were measured over a smaller range of extents (540 m -3 km). Colonization was negatively associated with the proportion of open-herbaceous cover and the density of roads, suggesting that habitat quality for *P. glaucus* decreases as forest fragmentation increases. The proportion of wetland cover also had a consistent positive association with extinction of *P. glaucus*. This study suggests that colonization and extinction of *P. glaucus* and *E. marcellus* are associated with ecological processes and land use at extents of kilometers.

TABLE OF CONTENTS

Acknowledgments	ii
Chapter 1. Factors affecting temporal variation in occupancy of two common species of butterflies in woodlands of the eastern United States, <i>Papilio glaucus</i> and <i>Eurytides marcellus</i> .	1
INTRODUCTION	2
METHODS	6
RESULTS	17
DISCUSSION	20
Literature Cited	26
Tables	37
Figures	39
Appendices	46

ACKNOWLEDGMENTS

I would like to thank a number of people who have helped me throughout this process. I extend my gratitude to my advisor, Dr. Matthias Leu, who was consistently patient throughout my three years at William and Mary and was always willing to help and offer advice. His positive attitude and good humor kept me motivated and always in good spirits. I also thank my graduate committee, Dr. Erica Fleishman, Dr. Jonathan Allen, and Dr. Harmony Dalglish, for their advice and suggestions, which have greatly improved the quality of my work.

There were a number of people that played an integral part in this project through their assistance with data collection in the field. In particular, I would like to thank Morgan Thompson, Elena Bishak, and Joey Thompson for giving up their summers to chase butterflies with me. Without their help, I would have never been able to accomplish the work that I have done.

Financial support for this project was provided by Strategic Environmental Research and Development Program (RC-2202).

Finally, I would like to express deep gratitude to my friends for making my graduate experience memorable. I am also tremendously grateful to my family for their unwavering support throughout not only this adventure but many before it, and hopefully many after.

Factors affecting temporal variation in occupancy of two common species of butterflies
in woodlands of the eastern United States, *Papilio glaucus* and *Eurytides marcellus*

INTRODUCTION

Each stage in a butterfly's life cycle requires different resources that can be characterized at different spatial and temporal scales (Scott 1992). The distribution of larval host plants, nectar sources, and minerals in soils affect the abundance and species richness of butterflies (Ehrlich and Raven 1965, Grossmueller & Lederhouse 1987, Hill 1992, Fischer et al. 1999, Aukland et al. 2004, Fleishman et al. 2005). Multiple studies directly addressed the strength of association between abundance, density, or occurrence and either host plants (Kjar and Barrows 2004, Breid et al. 2012) or nectar sources (Holl 1995, Shultz and Dlugosch 1999). However, few studies have examined strength of association between these response variables and the interactions between larval and adult resources. Dennis et al. (2006) highlighted the relevance of defining habitat on the basis of resources beyond larval host plants.

The composition and configuration of vegetation can affect the behavior and movement of butterflies. Open spaces with early successional vegetation may be a valuable resource for butterflies that search for mates on hilltops or by patrolling (Scott 1974, 1994). Habitat fragmentation also can affect the movements of butterflies (Hanski 1994, Haddad 1999, Hill et al. 2001, Schultz & Crone 2001, Tewksbury et al. 2002, Dennis et al. 2013). Haddad (1999) suggested that connectivity among forest patches facilitates dispersal of forest species, such as *Junonia coenia* and *Euptoieta claudia*, between forest patches. Species that disperse over relatively long distances may be able to traverse non-forested areas between habitat patches.

Land use may affect the distributions of butterflies at multiple scales (Rooney 2009, Staudt et al. 2013). Small disturbances often can lead to invasion by non-native plant species that alter resource availability for butterflies (Burghardt et al. 2009, Tallamy et al. 2009). A study of arthropod diversity in the mid-Atlantic region of the United States found that the composition of insects and other arthropods was different in sites dominated by native plants and sites dominated by non-native plants (Kjar and Barrows 2004). In much of the eastern United States, the composition and structural diversity of vegetation is increasingly affected by extensive urban development, which increases habitat quality for white-tailed deer (*Odocoileus virginianus*) populations that locally alter floral and faunal diversity via browsing (Côté et al. 2004).

The most commonly used methods to study effects of habitat change on population dynamics or distributions of butterflies are mark-release-recapture (Ehrlich and Davidson 1960), distance sampling (Buckland et al. 1993), and transect walks (Pollard & Yates 1993). Mark-release-recapture (MRR) methods facilitate monitoring of movement patterns, population size, and density (Thomas et al. 1996, Boughton 1999, Fischer et al. 1999, Schultz and Dlugosch 1999, Schultz and Crone 2001, Haddad et al. 2008). Distance sampling is a relatively new method and although it may work well for estimating the density of some vertebrates (Thomas et al. 2010), butterflies are often observed while in flight, which violates the assumptions of distance sampling where the individual must be recorded at a stationary point (Buckland et al. 1993). Transect walks are minimally invasive and generally require less time and resources to conduct than MRR. Unlike MRR, the transect-walk method cannot be used to estimate population size

or density, but allows estimation of abundance indices, is effective for monitoring common species over large areas (Haddad et al. 2008), and can be used to estimate occupancy, the probability that a species is present in an area after accounting for imperfect detection (MacKenzie et al. 2006). In this study I used transect walks to estimate occupancy, including turnover, of *P. glaucus* and *E. marcellus* from 2012 through 2015.

Use of occupancy models versus a naïve estimate of the proportion of sites occupied decreases biases in estimation by accounting for imperfect detection (MacKenzie et al. 2006), or the probability that a species is detected given that it is present. Although it is relatively easy to establish that a species is present at a site, it is more difficult to determine that a species is absent. For example, sampling conditions and observer perceptions can lead to false absences. Occupancy models use detections histories, or a series of presence (1) and absence (0) records across multiple sampling occasions (surveys), to estimate occupancy and other parameters. Probabilities of different presence and absence histories are used to determine detection probability (MacKenzie et al. 2006). Heterogeneity in occupancy among sites can be modeled on the basis of variables that represent ecological processes at different spatial extents. Model parameters are estimated with logit link functions, with parameter values ranging from 0 to 1 (MacKenzie et al. 2006). The five assumptions of occupancy modeling are: occupancy remains constant throughout a given season, or changes in occupancy are appropriately modeled; probability of detection remains constant, or changes in probability of detection are appropriately modeled; detections of individuals at each site

are independent; species are not falsely detected; and occupancy status does not change among surveys (closure assumption, MacKenzie et al. 2006).

Occupancy can be estimated on the basis of either single-season or multi-season models. Multi-season models estimate not only detection probability and occupancy, but also the probability of extinction and colonization across multiple seasons (MacKenzie et al. 2006). Seasons can be defined as years or other intervals of time depending on the focus of the study. Colonization is defined as the probability that a site was unoccupied in the previous season is occupied in the current season. Conversely, extinction is defined as the probability that a site is unoccupied in the current season given that it was occupied in the previous season. Between seasons, a site can be colonized, become vacant, remain occupied, or remain unoccupied. In this context, colonization and extinction of butterflies are probabilities of turnover (Hanski 1994).

Occupancy models largely have been applied to vertebrates (Adams et al. 2013, Tobin et al. 2014, Hayes and Monfils 2015). Few studies have modeled occupancy of insects. In temperate ecosystems, most butterfly species can be detected and identified fairly easily in the field. Most estimates of the occupancy of butterflies were on the basis single-season models (Pellet 2008, van Strien et al. 2011, Bried et al. 2012, Roth et al. 2014). Few studies used occupancy models to relate probabilities of colonization and extinction of butterflies to ecological processes (but see Fernández-Chacón et al. 2014).

The objective of my study was to explore occupancy of two species of butterflies that are common in woodlands in the Chesapeake Bay Lowlands, *Eurytides marcellus* and *Papilio glaucus*. I explored the extent to which temporal variation in occupancy,

colonization, and extinction was associated with temporally varying distributions and abundances of nectar sources and stationary densities of host plants.

METHODS

Study area

This study was conducted in the Chesapeake Bay Lowlands of southeastern Virginia near the cities of Williamsburg, Newport News, and New Kent. Within this area, complex river systems form peninsulas that delineate the coastline of the Chesapeake Bay. The study area spanned the Middle and Virginia peninsulas, which are bordered by the James River, the York River, and their tributaries. Coniferous forests in the area are dominated by loblolly pine (*Pinus taeda*) and deciduous forests are dominated by American beech (*Fagus grandifolia*), white oak (*Quercus alba*), tulip poplar (*Liriodendron tulipifera*), and hickory (*Carya* spp.). Hickory and oak (*Quercus* spp.) are more common in upland forests. Riparian and floodplain forests contain sweet gum (*Liquidambar styraciflua*), red maple (*Acer rubrum*), tulip poplar (*Liriodendron tulipifera*), and American sycamore (*Plantanus occidentalis*). Common mid-story plants include flowering dogwood (*Cornus florida*), arrowwood (*Viburnum dentatum*), American holly (*Ilex opaca*), and mountain laurel (*Kalmia latifolia*). The understory is diverse, but large areas can become dominated by huckleberries and blueberries (*Vaccinium* spp.) (Monette and Ware 1983).

Study species

Eurytides marcellus is a common woodland butterfly species in the eastern United States. This species typically is bivoltine, but in areas of the southern United States it has

three or four broods per flight season (Opler and Krizek 1984). The flight period for this species typically starts in April and ends mid-September. Unlike *P. glaucus*, *E. marcellus* is oligophagous; females lay their eggs on *Assimina* spp. The most common host plant of *E. marcellus* in most of its range is common pawpaw (*Assimina triloba*), which typically grows in rich, mesic soils and is uncommon in old growth forests and early successional forests (Willson and Schemske 1980). In some areas in southern North Carolina, *E. marcellus* also lays eggs on *A. lonifolia*, *A. parviflora*, *A. pygmaea*, *A. reticulata*, and *A. speciosa*, but these species are not common in the study area (Opler and Krizek 1984). Little information is available about the oviposition behavior and movement patterns of *E. marcellus*. The species is a generalist nectar feeder but has a shorter proboscis than other Papilioninae, and therefore cannot take nectar from flowers with long corollas (Opler and Krizek 1984). In the early spring, nectar sources include blueberry, redbud (*Cercis canadensis*), and black cherry (*Prunus serotina*). Later in the season, nectar sources include milkweed (*Asclepias* spp.), dogbane (*Apocynum* spp.), and sweetpepper bush (*Clethra alnifolia*) (Opler and Krizek 1984, A. Zappalla pers. obs.).

Papilio glaucus is common in eastern deciduous woodlands east of the Rocky Mountains from Canada to Florida. Although the number of broods varies among regions, *P. glaucus* in the Chesapeake Bay Lowlands have two broods, with adults flying throughout mid-spring and late summer (Hagen and Lederhouse 1985, Scott 1996, Wagner 2005). In the study area, *P. glaucus* commonly begins flying around mid-April (L. Tafoya, pers. com.). Across its range *P. glaucus* can oviposit on a number of different trees in different families, but females in the eastern United States most commonly

oviposit on *Magnoliaceae* and *Rosaceae*, particularly *L. tulipifera*, *Prunus serotina*, *Fraxinus americana* and *Magnolia virginiana* (Sciber 1986, Wagner 2005, L. Tafoya, pers. com.). Females usually lay their eggs 3 m above ground, orienting eggs to maximize sunlight exposure throughout development (Grossmueller and Lederhouse 1983). Adult butterflies take nectar from a variety of flowering plants, but usually from plants ≥ 1.5 m above ground. They also have been observed taking nectar from shrubs with low-hanging branches and herbaceous plants that are less than 1.5 m above ground (Opler and Krizek 1984, A. Zappalla pers. obs.). Common nectar sources for *P. glaucus* include milkweed, thistle (*Cirsium* spp.), honeysuckle (*Lonicera* spp.), ironweed (*Vernonia* spp.), Joe-Pye weed (*Eutrochium* spp.) (Opler and Krizek 1984), and plants in the *Apocynaceae*, *Asteraceae*, *Caprifoliaceae*, *Oleaceae*, and *Rubiaceae*.

Survey Design

Occurrence data for both species were collected on 65 500-m transects on the basis of modified transect walks (Pollard and Yates 1992) from 2012 through 2015. I recorded all butterflies detected within 5 m on either side of the transect (Pollard and Yates 1992) while walking at a slow speed; the average time to walk both directions along a transect was around 30 min. Each transect was sampled six times (every two weeks) from mid-May through mid-August. Transects were sampled between 0900 and 1700 and were not sampled on rainy or windy days (Pollard and Yates 1992).

Starting points of transects were located at random along forest gravel roads and trails. Transects were placed on lands managed by the Virginia Department of Forestry (Dragon Run State Forest, $n = 7$; Sandy Point State Forest, $n = 4$), Department of Inland

Fish and Game (Chickahominy Wildlife Refuge, $n = 8$), City of Gloucester Courthouse (Beaverdam State Park, $n = 5$), City of Newport News (Newport News Park, $n = 16$), City of Williamsburg (College Woods, $n = 10$; Colonial Williamsburg, $n = 4$), York County (New Quarter Park = 4), and the United States Army (Joint Base Langley-Eustis, $n = 7$). The coordinates of the endpoints of transects were recorded with a global positioning system (GPS). Transects were stratified among the major land-cover types within the study area: riparian, mesic forest, and upland dry forest.

Survey-specific Variables

To model potential heterogeneity in detection probability, I measured survey-specific environmental variables known to affect the presence of butterflies. I measured wind speed (m/s) and temperature ($^{\circ}\text{C}$) with a hand-held weather station (Kestrel 200, A Weather Republic, Downingtown, PA). Because rainfall affects both butterfly flight and nectar availability, I estimated the number of days since rain for a given survey date and location. I collected dates of rainfall from weather stations at Felker Army Air Field, Middle Peninsula Regional Airport, Williamsburg/Jamestown Airport, and Newport News/Williamsburg International Airport. I used ArcGIS 10.2 (ESRI 2014) to identify the airport closest to each transect.

Site-specific Variables

I selected variables that I hypothesized *a priori* would explain occupancy, colonization, and extinction of both species. I modeled heterogeneity in these parameters on the basis of variables measured in the field or remotely at different spatial extents and resolutions (Table 1).

Field measurements

On all transects, I recorded categorical abundance of flowering plants (i.e., plants that might serve as sources of nectar for either species) within 5 m of transects (0 = none, 1 = one or two, 2 = more than two and less than seven, 3 = more than seven) (Fischer et al. 1999, Fleishman et al. 2002). I predicted that abundance of nectar would be positively associated with detection probability, colonization, and extinction.

To characterize the density and basal area of potential host plants on and near transects I conducted vegetation surveys in 2014. I used ArcGIS 10.2 (ESRI 2014) to select three random points within a 90-m buffer around each transect and uploaded the coordinates of these points to a GPS (GPSMAP 62; Garmin, Olathe, Kansas, USA). Each point served as the center of two nested plots with radii of 7.5 m and 15 m. In the 15-m radius plot, I counted and measured the diameter at breast height (dbh) of all trees in the canopy (tallest trees) and subcanopy (below the tallest trees) that potentially could serve as larval hosts and had a dbh of > 10 cm. From these measurements, I then calculated the basal area of the trees totaled across all three sample plots. I identified potential host plants to species and all other trees to genus or order. For *P. glaucus*, I measured *L. tulipifera*, *P. serotina*, and *M. virginiana* as the host plants based on regional preference (Scriber 1986, Wagner 2005). In the 7.5-m radius plot, I identified and counted the number of shrubs and saplings that potentially could serve as larval hosts and had a dbh ≥ 1 cm and ≤ 10 cm. All densities and basal area measurements were summed for all three sampling plots. I predicted that host plant density at varying canopy heights and basal

area and density of deciduous trees would be positively associated with occupancy for *P. glaucus*.

Because *A. triloba* mostly occurs as saplings < 1 m tall and < 1 cm dbh, I used the line intercept method to estimate the proportion of cover for that species. I centered two 30-m lines, one running north–south and one running east–west, on the midpoint of the vegetation plot. For every one meter interval along each 30-m transect, I recorded if the plant intersected the transect line, which I then used to get a proportion of the total intersections out of 59 meters (the center meter was only counted once). I predicted that proportion of cover of *A. triloba* would be positively associated with occupancy for *E. marcellus*.

I examined the association of canopy height and structural heterogeneity with colonization and extinction on the basis of discrete-return light detection and ranging (LiDAR) data (Table 1) LiDAR data were extracted within 90-m buffers around each butterfly transect (Table 1). LiDAR data have been used to quantify the vertical distribution of plant biomass (Vierling et al. 2008) and therefore is well suited to evaluate the effects of deer browsing. LiDAR data were collected from 22 April – 10 May 2010, and 21 – 31 March, 2013; I acquired these data from a public-access repository (virginalidar.com 2015). I used LAStools software (version 150202; <http://lastools.org>) to process the LiDAR data and to derive canopy height and structural heterogeneity at 10 m² resolution. Structural heterogeneity from 0.3–3 m above ground was calculated as the number of returns divided by the number of laser signals emitted per 10 m² cell (Morsdorf et al. 2006). I removed low-altitude LiDAR points (< 0.3 m) to avoid noise

from forest floor vegetation. I predicted that estimates of canopy height and structural heterogeneity would be positively associated with extinction of *E. marcellus* because its host plant grows in forest stands that have a semi-open understory (Sullivan 1993). I predicted that *P. glaucus* would be associated positively with canopy height and structural heterogeneity because one of its host plants, *L. tulipifera*, is dominant in the canopy and understory.

Remotely sensed measurements

To determine how occupancy, colonization, and extinction might be influenced by a broader extent of resource availability, I measured land-cover variables that might serve as proxies for the abundance of host plants, mineral sources, and nectar sources (Table 1). Given the known host plants for both species, I hypothesized that the proportion of mesic forest and riparian forest would be positively associated with colonization and the proportion of wetland and coniferous forest would be positively associated with extinction. I hypothesized that the proportion of floodplain forest and upland forest land cover would be positively associated with colonization of *P. glaucus* and extinction of *E. marcellus*. The highest-quality habitat of *A. triloba* is mesic woodlands that have moist soils, but are not regularly inundated with water (Sullivan 1993). The host plants for *P. glaucus* grow well in both upland and mesic forests; *L. tulipifera* is flood-tolerant in coastal southeastern ecosystems (Parks et al. 1994). Riparian forests also provide wet soils from which males of both species obtain minerals (Arms et al. 1974, Scott 1992). I hypothesized that the proportion of wetland and coniferous woodland would be

negatively associated with occupancy of both species given the biology of their host plants.

Nectar sources commonly visited by both species are herbaceous plants that typically grow in recently disturbed areas or along edges (Opler and Krizek 1984). Land-cover and land-use types with high levels of disturbance include early successional forest, open herbaceous, and agriculture. I measured proportion of agriculture because in the study area agricultural areas typically are surrounded by herbaceous plants (Jonsen and Fahrig 1997, Flick et al. 2012, A. Zappalla pers. obs). I related probability of extinction and colonization to the density of edges between mixed deciduous and coniferous-mixed deciduous forests (henceforth referred to as forests) and between agriculture and open herbaceous (Table 1). Edges between woodlands and agriculture often have high densities of flowering herbaceous plants (Flick et al 2012). In addition, both *P. glaucus* and *E. marcellus* are large-bodied butterflies that fly along edges and across open fields to patrol for mates and to locate food sources or sites for oviposition (Opler and Krizek 1984). Because edges likely do not act as a barrier to movement of either species, I hypothesized a positive association between colonization and the density of edges between forests and areas that have the potential for high nectar.

I also used road density (km/km^2) as a proxy for nectar abundance (Ries et al. 2001, Matteson et al. 2013). I used a Wilcoxon signed-rank test to evaluate whether the abundance of nectar, measured as median nectar score, was higher along roads than along interior forest transects. Median nectar scores were significantly higher on road transects than forest transects ($W = 17$, $p = 0.01$, $n = 20$). The roads included in the analysis

encompassed two classes of which were either local or other. Local roads are defined as neighborhood and rural roads and other roads are defined as, highway ramps, service roads, alleys, private roads, and parking lot roads (US Census Bureau 2015).

I calculated the proportion of different land-cover types and the density of edges and roads at five extents (i.e., buffers surrounding each transect): 270 m, 540 m, 1 km, 3 km, and 5 km. I selected these extents on the basis of known movement distances of *P. glaucus*, which extend to 5 km (Fales 1959, Scott 1975, Lederhouse 1982, Grossmueller and Lederhouse 1987, Scott 1992). Because I could not find any data on movements of *E. marcellus*, I used the same extents. In ArcGIS 10.2 (ESRI 2014), I extracted LANDFIRE (www.landfire.gov) data on the proportion of each cover type. I combined LANDFIRE Existing Vegetation Types (EVTs) that fell within the same land-cover class (Appendix 1). I derived the density of edges between the land-cover types described above in Geospatial Modeling Environment (Beyer 2011). I extracted data on roads from the Topologically Integrated Geographic Encoding and Referencing (TIGER) data (<http://www.census.gov/>).

Modeling Approach

To estimate occupancy, colonization, and extinction I used multi-season open models (Chambert et al. 2015). I defined season as the flight period (late spring and summer) in each year.

Because both species are highly vagile and likely move throughout the study area in a non-random way, the closure assumption of multi-season occupancy models likely was violated (MacKenzie et al. 2006). To test whether the assumption was violated, I first

ran both closed (MacKenzie et al. 2006) and open multi-season occupancy models (Chambert et al. 2015). The open multi-season model estimates probabilities of entry and departure of each species from each sampling location (in this case, transect) (Chambert et al. 2015). The model assumes that the species does not enter or exit the transect more than once during the season (Kendal et al. 2013, Chambert et al. 2015). Because the entry and exit probabilities were not a focus of my research, I included them as constants in all models.

After I identified whether an open or closed model was more strongly supported by the data, I used univariate and multivariate models to evaluate the strengths of association between covariates and detection probability, occupancy, colonization, and extinction. I centered and standardized all variables so that their slopes could be compared directly. For each variable, I tested linear, quadratic ($x+x^2$), and pseudo-threshold ($\ln[x]$) functions. I used Akaike's Information Criterion (AIC_c) (ΔAIC and AIC model weight) adjusted for small samples sizes to determine which models were best supported by the data (Burnham and Anderson 2002).

The first step in the model-selection process was to determine which survey-specific variables—season, season and sampling occasion (additive; I set occasion 6 as the intercept), the interaction between season and survey, and nectar abundance—explained the greatest proportion of variance in detection probability. I grouped nectar abundance into low (score of 0, 1, and 2) and high (3) classes on the basis of the maximum nectar score across the season. I did not differentiate scores of 0 because there were few transects on which no nectar was recorded. All survey-specific variables were

carried forward in the modeling process if the AIC of the models in which they were included was lower than that of the null model (detection probability held constant) and if the models in which they were included provided robust estimates of the regression coefficients (standard errors < 3). I calculated p^* , the probability of observing a given species at least once during a given season (MacKenzie et al. 2006). Estimation of occupancy, colonization, and extinction becomes difficult when $p^* < 0.85$ (MacKenzie et al. 2006). I used the best-supported model of detection probability as the null model when estimating occupancy, extinction, and colonization.

I first ran univariate models to identify the spatial extent and functional form (linear, quadratic, or pseudo-threshold) that explained the greatest proportion of variance in occupancy, colonization, and extinction. I used two types of design matrices in univariate models. One included an intercept and a year effect, and the other included an intercept and effect size, which I included as an additional intercept to offset the effect between seasons when either naïve extinction or colonization was ≤ 2 events. A variable was retained if the estimates of the regression coefficients were plausible (i.e., estimates ranged from -5 to $+5$ and SEs < 3). If the AICs of multiple univariate models were within $2 \Delta AIC$ and the linear model was among these, I retained the linear model because linear associations between response variables and covariates generally are easier to interpret than nonlinear associations. I used the “cor function” in R (R Core Team 2013) to run Spearman rank correlations (r_s) between all pairs of covariates. I did not include any variables with $r_s > |0.60|$ in the same model (Leu et al. 2011).

To estimate final colonization and extinction parameters, I ran models that included all possible combinations of variables retained from the candidate set, with the best-supported occupancy and detection models included. I limited the number of variables included in each model to $\leq 10\%$ of the number of transects (i.e., ≥ 6 variables per model) to avoid overfitting (Hosmer and Lemeshow 2000). I derived final estimates of the regression coefficients and standard errors from the most strongly supported models that summed to an AIC weight of 0.95 (Burnham & Anderson 2002). I used conditional model averaging to estimate regression coefficients and unconditional model averaging to estimate standard errors of the slopes. I compared model AIC weights among variables to evaluate the strength of evidence that each was associated with colonization or extinction (Burnham & Anderson 2002).

The multi-season models generated estimates of occupancy in 2012 and of colonization and extinction from 2012 to 2013, 2013 to 2014, and 2014 to 2015. I used the estimates of colonization and extinction to estimate occupancy in 2013, 2014, and 2015. I estimated annual variance in occupancy on the basis of the delta method. All modeling was done in PRESENCE (Hines 2006). For all parameter estimates, unless otherwise noted, I report values \pm SE.

RESULTS

In each year, *E. marcellus* and *P. glaucus* were detected on at least one transect. Naïve occupancy of *E. marcellus* from 2012-2015 remained relatively consistent: 0.43, 0.46, 0.40, and 0.43, respectively. By contrast, naïve occupancy of *P. glaucus* in each year was 0.33, 0.85, 0.29, and 0.51, respectively.

For both species, the open multi-season model fit the data better than the closed multi-season model ($> 10 \Delta AIC$ for both species) (Appendix 2). The most strongly supported model of detection of *E. marcellus* included an interaction between season and survey and the number of days since rain (Appendix 3). The number of days since rain was positively associated with detection probability ($\beta = 0.27 \pm 0.11$). The probability of detecting *E. marcellus* at least once did not vary from 2012-2015 (Fig. 1). The most strongly supported model of detection of *P. glaucus* included the additive effect of season and survey (Appendix 4) with no additional variables. Although a model that included nectar abundance had a lower AIC than the season + survey model, I excluded the nectar variable because its inclusion created problems for estimation of colonization and extinction. The probability of detecting *P. glaucus* at least once varied among years (Fig. 1).

Univariate Models

The most strongly supported univariate model of the occupancy of *E. marcellus* in 2012 included the proportion of *A. triloba* ($\beta = 5.80 \pm 2.97$) (Appendix 5). The best-supported univariate model of the occupancy of *P. glaucus* in 2012 included the number of potential host plants ($\beta = 0.64 \pm 0.47$) (Appendix 6).

The most strongly supported univariate model of colonization of *E. marcellus* included the proportion of agriculture within 270 m ($\beta = 1.09 \pm 0.47$) and a quadratic function of the density of edges between forests and open herbaceous within 3 km ($\beta x = 2.75 \pm 1.30$, $\beta x^2 = -2.59 \pm 0.99$) (Appendix 7). The two most strongly supported univariate models of colonization of *P. glaucus* included the proportion of open

herbaceous within 3 km ($\beta = -1.95 \pm 0.83$) and the density of neighborhood and rural roads within 3 km ($\beta = -1.78 \pm 0.75$) (Appendix 8).

Two variables were included in the most strongly supported univariate models of extinction of *E. marcellus*: the density of edges between forests and wetlands within 5 km ($\beta = -1.87 \pm 0.70$) and structural heterogeneity of vegetation within 90 m, ($\beta = 0.96 \pm 0.36$) (Appendix 9). Three variables were included in the most strongly supported univariate models of extinction of *P. glaucus*: density of edges between forests and wetlands within 540 m ($\beta = 1.31 \pm 0.52$), proportion of wetlands within 3 km ($\beta = 4.63 \pm 3.85$), and proportion of coniferous forest within 1 km ($\beta = -3.29 \pm 2.42$) (Appendix 10).

Multivariate Models

Six models of colonization and extinction of *E. marcellus* summed to an AIC weight of 0.95 (Appendix 11). The variable that explained the greatest proportion of variance in colonization was the density of edges between forests and open herbaceous within 3 km (Fig. 2). Probability of colonization peaked at 3.5 km/km² (Fig. 3). The proportion of agriculture within 270 m also was positively associated with probability of colonization (Fig. 2). Probability of colonization increased exponentially at a threshold of roughly 10% agricultural cover within 270 m (Fig. 3). The density of edges between forests and wetlands within 5 km explained the greatest proportion of variance in probability of extinction (negative association) (Fig. 2). The probability of extinction approached zero asymptotically at roughly 1.2 km/km² (Fig. 3). The structural heterogeneity of the understory was positively and linearly associated with probability of extinction (Fig. 2).

Ten models of colonization and extinction of *P. glaucus* summed to an AIC weight of 0.95 (Appendix 12). Proportion of agriculture within 3 km explained the greatest proportion of variance in probability of colonization (Fig. 2). Probability of colonization declined as the proportion of agriculture rose above 0.05 (Fig. 4). The density of local roads, especially at densities $> 2 \text{ km/km}^2$, was negatively associated with colonization (Fig. 4). Density of edges between forests and wetlands within 540 m was most strongly (and negatively) associated with probability of extinction (Fig. 2). Probability of extinction approached 1.0 asymptotically around 2 km/km^2 (Fig. 4). The probability of extinction increased linearly as the density of edges between mixed-deciduous forest and wetland within 3 km increased (Fig. 4). Proportion of wetland within 3 km was positively (Fig. 2) and sigmoidally associated with extinction probability, which approached 1.0 around 0.10 wetland cover (Fig. 4). The proportion of coniferous forest within 1 km was negatively associated with extinction (Fig. 2). Probability of extinction approached zero at around 0.20 coniferous cover (Fig. 4).

Occupancy of *E. marcellus* was relatively stable from 2012 through 2015 (Fig. 5). Occupancy of *P. glaucus* was less consistent, doubling between 2012 and 2013 and dropping in 2014 (Fig. 5).

DISCUSSION

The open multi-season model (Chambert et al. 2015) explained more variance in occupancy of both *P. glaucus* and *E. marcellus* than the closed multi-season model (MacKenzie et al. 2006). This result is consistent with the known movement distances and phenology of both species, which are highly vagile and have multiple broods (Fales

1959, Scott 1975, Grossmueller and Lederhouse 1987, Lederhouse 1982, Scott 1992).

With an open model, one can identify factors that are associated with entry into and departure from study sites. However, I was not able to estimate these parameters because I did not sample before the species' entry and after their departure from the study sites (Chambert et al. 2015).

To better understand the dynamic occupancy patterns of both species, I used potential proxies for the abundance of host plants and nectar sources at multiple extents and measurements of site level host plant and nectar availability (Thomas et al. 2001, Fleishman et al. 2002). The most strongly supported models suggested that the greatest proportion of variance in occupancy in 2012 was explained by the availability of host plants (Appendix 2 and 3). There were no associations between nectar and colonization or extinction for the site level nectar score variable in both species. The proxies for nectar were only important for *E. marcellus* with positive associations between open herbaceous and agriculture land cover variables and colonization. This result suggests that the variables measuring nectar in this study were not as important as predicted to explain variation in colonization and extinction. These findings are corroborated by a study on butterfly movement in reclaimed coal mine forests in southwestern Virginia, where nectar influenced the local movement of individuals but not dispersing individuals (Holl 1995). I found that for *P. glaucus* nectar was not an important variable explaining heterogeneity in occupancy but was important explaining variation in the detection probability, which suggests that having more nectar on transects increased detection of this species (Appendix 3). In contrast, Fleishman et al. (in review) found that heterogeneity in

butterfly occupancy in western montane ecosystems, among other variables, was explained by variation in nectar resources. The distribution of nectar sources in my sites were relatively clumped, leading potentially to an underestimation of nectar.

I found that the proportion of open-herbaceous vegetation and agriculture was positively associated with colonization of *E. marcellus*. The density of edges between forest and open-herbaceous vegetation explained the greatest proportion of variance in colonization. The latter relation was quadratic, which may reflect greater availability of nectar but lower availability of *A. triloba* near edges. *A. triloba* does not grow well in forest stands with the high-density understory (Willson and Schemske 1980) that typically occurs near edges. Additionally, the probability of extinction of *E. marcellus* increased as structural heterogeneity of vegetation within 90 m of transects increased (Figure 4). With increased fragmentation of forest and decreased patch sizes, the quality of habitat might degrade to a point where the host plant is no longer present in the landscape leading to a decline in colonization (Fernández-Chacón et al. 2014). This could potentially be the case for *A. triloba*, where the quality of the habitat becomes degraded to a point where the host plant is no longer present, but more research is needed to support this assumption.

The proportion of open herbaceous vegetation within 3 km explained the greatest proportion of variation in colonization of *P. glaucus*, and the association was negative. I assumed that the proportion of herbaceous vegetation functioned as a proxy for nectar availability (Opler and Krizek 1984). Either my assumption may have been erroneous, or nectar availability may not explain much variation in colonization (Holl 1995).

Moreover, I found that probability of colonization decreased substantially as the density of local roads, and presumably forest fragmentation, increased. Density of roads may be correlated with availability of nectar. It also is possible that mortality of adults increases as road density increases (Ries et al. 2001). All of the variables that were positively associated with extinction of *P. glaucus* were related to the configuration of wetlands. Wetlands likely contain few host plants. Although *L. tulipifera* is flood tolerant (Parks et al. 1994), it does not thrive in wetlands.

The 95% confidence intervals for the majority of regression coefficients included zero. Although this suggests that the associations between response variables and environmental variables were weak, models that included these environmental variables explained more variance in the response variables than the null model. It is unclear whether model fit will improve when temporal variation in entry and departure is included.

My study suggests that when studying population dynamic in butterflies, the open-population multi-season occupancy model (Chambert et al. 2015) has the potential to be an excellent alternative approach to mark-release-recapture (MRR) (Thomas et al. 1996) and distance sampling (Thomas et al. 2010). However there are three caveats to consider. First, it is important to adjust naïve occupancy estimates by imperfect detection (MacKenzie et al. 2006). The difference in naïve and detection-weighted estimates of occupancy of *P. glaucus* were substantial in 2014. Naïve estimates suggested that occupancy in 2014 was considerably below that in other years. The difference was less marked in detection-weighted estimates of occupancy. Second, sampling effort needs to

be adjusted annually depending on the population density of the butterfly species studied. I found when turnover in occupancy was high, variation in p^* was also high. Estimates for p^* in 2012 and 2013 were > 0.85 , but dropped to < 0.5 in 2014. The apparent dynamics of *P. glaucus* complicated estimation of occupancy, extinction, and colonization. Therefore when estimating occupancy, colonization, and extinction in years with relatively low occupancy, additional survey are required to capture homogenous detection histories that allow robust estimation of parameters. Third, the open-population multi-season model offers an opportunity to model variation in entry and exit probabilities (Chambert et al. 2015). To model these parameter, sampling designs need to include surveys outside of the typical flying period of a given butterfly species. With the increased interest on how climate change affects butterfly population (Breed et al. 2013, Parmesan et al. 2013, Radchuk et al. 2013) this method offers an opportunity to assess how butterfly species respond to current climate condition that can be implement to forecast distributions under various future climate scenarios.

Future conservation and management projects that aim to improve butterfly habitat can use these results as a guide to understanding the effects of resource availability and landscape structure on these species. While the findings show that these butterflies have a tolerance for landscape heterogeneity, they highlight potential features of the landscape that can drive down colonization. These include increased edges between land cover types for *E. marcellus* and increased density of roadways for *P. glaucus*. Both of these land use features are common in highly developed human landscapes and while both of these species are tolerant to human disturbances (Di Mauro

et al. 2007, A. Zappalla per. obs.) this study shows that these stressors have the potential to drive down colonization. Another important take away for the management of butterfly habitat is the extent at which these species are affected. Both species exhibited significant associations with landscape variables that were more than a kilometer away from the sampling location. While it is important to maintain the quality of the local habitat, the surrounding landscape must also be considered since both of these species have the potential to move large distance in the course of a day. By accounting for the dynamic use of habitat for these two species, better management practices can be implemented to ensure that projects lead to long term site occupancy by these two species.

LITERATURE CITED

- Adams, M.J., Miller, D.A., Muths, E., Corn, P.S., Grant, E.H.C., Bailey, L.L., Fellers, G.M., Fisher, R.N., Sadinski, W.J., Waddle, H. and Walls, S.C. 2013. Trends in amphibian occupancy in the United States. *PloS ONE*, 8:p.e643-647.
- Arms, K., Feeny, P., and Lederhouse, R.C. 1974. Sodium: stimulus for puddling behavior by tiger swallowtail butterflies, *Papilio glaucus*. *Science* 185:372-374.
- Auckland, J.N., Debinski, D.M., and Clark, W.R. 2004. Survival, movement, and resource use of the butterfly *Parnassius clodius*. *Ecological Entomology* 29: 139-149.
- Beyer, H.L. 2011. Geospatial Modeling Environment. URL <http://www.spataleecology.com/gme/index.htm> (accessed 7/24/2015).
- Boughton, D.A. 1999. Empirical evidence for complex source-sink dynamics with alternative states in a butterfly metapopulation. *Ecology* 80: 2727-2739.
- Breed, G.A., Stichter, S. and Crone, E.E. 2013. Climate-driven changes in northeastern US butterfly communities. *Nature Climate Change* 3:142-145.
- Bried, J.T., Murtaugh, J.E., and Dillon, A.M. 2012. Local distribution factors and sampling effort guidelines for the rare frosted elfin butterfly. *Northeastern Naturalist* 19:673–684.
- Buckland, S.T., Anderson, D.R., Burnham, K.P., and Laake, J.L. 2005. Distance sampling. John Wiley and Sons, Hoboken, New Jersey, USA.

- Burghardt, K.T., Tallamy, D. W., and Gregory Shriver, W. 2009. Impact of native plants on bird and butterfly biodiversity in suburban landscapes. *Conservation Biology* 23:219-224.
- Burnham, K.P., and Anderson, D.R. 2002. Model selection and multimodel inference: a practical information-theoretic approach. Springer Science and Business Media. New York, New York, USA.
- Chambert, T., Kendall, W.L., Hines, J.E., Nichols, J.D., Pedrini, P., Waddle, J.H., Tavecchia, G., Walls, S.C. and Tenan, S. 2015. Testing hypotheses on distribution shifts and changes in phenology of imperfectly detectable species. *Methods in Ecology and Evolution* 6:638-647.
- Côté, S.D., Rooney, T.P., Tremblay, J.P., Dussault, C., and Waller, D.M. 2004. Ecological impacts of deer overabundance. *Annual Review of Ecology, Evolution, and Systematics* 35:113-147.
- Dennis, R.L., Hodgson, J.G., Grenyer, R., Shreeve, T.G. and Roy, D.B. 2004. Host plants and butterfly biology. Do host-plant strategies drive butterfly status? *Ecological Entomology* 29:12-26.
- Dennis, R.L., Shreeve, T.G., and Van Dyck, H. 2006. Habitats and resources: the need for a resource-based definition to conserve butterflies. *Biodiversity and Conservation* 15:1943-1966.
- Dennis R.L.H, Dapporto L., Dover JW., and Shreeve T.G. 2013. Corridors and barriers in biodiversity conservation: a novel resource-based habitat perspective for butterflies. *Biodiversity and Conservation* 22:2709-2734.

- Di Mauro, D., Dietz, T. and Rockwood, L. 2007. Determining the effect of urbanization on generalist butterfly species diversity in butterfly gardens. *Urban ecosystems* 10:427-439.
- Ehrlich, P.R., and Davidson, S. E. 1960. Techniques for capture-recapture studies of Lepidoptera populations. *Journal of the Lepidopterists' Society* 14:227-229.
- Ehrlich, P.R., and Raven, P.H. 1964. Butterflies and plants: a study in coevolution. *Evolution* 18: 586-608.
- ESRI. 2014. ArcMap. Environmental Systems Research Institute, Redlands, CA.
- Fales, J.H. 1959. A field study of the flight behavior of the tiger swallowtail butterfly. *Annals of the Entomological Society of America* 52:486-487.
- Fernández-Chacón, A., Stefanescu C., Genovart M., Nichols J.D., Hines J.E., Páramo F., Turco M., and Oro, D. 2014. Determinants of extinction–colonization dynamics in Mediterranean butterflies: the role of landscape, climate and local habitat features. *Journal of Animal Ecology* 83:276–285.
- Fischer K., Beinlich B., and Plachter H. 1999. Population structure, mobility and habitat preferences of the violet copper *Lycaena helle* Lepidoptera: Lycaenidae in Western Germany: implications for conservation. *Journal of Insect Conservation* 3:43–52.
- Fleishman, E., C. Ray, P. Sjögren–Gulve, C.L. Boggs, and Murphy, D.D. 2002. Assessing the relative roles of patch quality, area, and isolation in predicting metapopulation dynamics. *Conservation Biology* 16:706–716.

- Fleishman, E., Mac Nally, R., and Murphy, D. D. 2005. Relationships among non-native plants, diversity of plants and butterflies, and adequacy of spatial sampling. *Biological Journal of the Linnean Society* 85:157-166.
- Flick, T., Feagan, S., and Fahrig, L. 2012. Effects of landscape structure on butterfly species richness and abundance in agricultural landscapes in eastern Ontario, Canada. *Agriculture, Ecosystems and Environment* 156:123-133.
- Grossmueller, D. W., and Lederhouse, R. C. 1985. Oviposition site selection: An aid to rapid growth and development in the tiger swallowtail butterfly, *Papilio glaucus*. *Oecologia* 66:68-73.
- Grossmueller, D. W., and Lederhouse, R. C. 1987. The role of nectar source distribution in habitat use and oviposition by the tiger swallowtail butterfly. *Journal of the Lepidopterists' Society* 41:159-165.
- Haddad, N. M. 1999. Corridor and distance effects on interpatch movements: a landscape experiment with butterflies. *Ecological Applications* 9:612-622.
- Haddad, N.M. and Tewksbury, J.J. 2005. Low-quality habitat corridors as movement conduits for two butterfly species. *Ecological Applications* 15:250-257.
- Haddad, N.M., Hudgens, B., Damiani, C., Gross, K., Kuefler, D., and Pollock, K. 2008. Determining optimal population monitoring for rare butterflies. *Conservation Biology* 22:929-940.
- Hagen, R.H. and Lederhouse, R.C. 1985. Polymodal emergence of the tiger swallowtail, *Papilio glaucus* Lepidoptera: Papilionidae: Source of a false second generation in central New York State. *Ecological Entomology* 10:19-28.

- Hanski, I. 1994. Patch-occupancy dynamics in fragmented landscapes. *Trends Ecology and Evolution* 9:131–135
- Hayes, D.B. and Monfils, M.J. 2015. Occupancy modeling of bird point counts: Implications of mobile animals. *The Journal of Wildlife Management*, 79:1361-1368.
- Hill, J.K., Thomas, C.D., and Lewis, O.T. 1996. Effects of habitat patch size and isolation on dispersal by hesperia comma butterflies: Implications for metapopulation structure. *Journal of Animal Ecology* 65:725-735.
- Hill, J.K., Collingham, Y.C., Thomas, C.D., Blakeley, D.S., Fox, R., Moss, D., and Huntley, B. 2001. Impacts of landscape structure on butterfly range expansion. *Ecology Letters* 4: 313-321.
- Hines, J.E. 2006. PRESENCE – software to estimate patch occupancy and related parameters. US Geological Survey – Patuxent Wildlife Research Center. www.mbr-pwrc.usgs.gov/software/presence.html (accessed 3/25/2016).
- Holl, K.D. 1995. Nectar resources and their influence on butterfly communities on reclaimed coal surface mines. *Restoration Ecology* 3:76-85.
- Hosmer, D.W., and Lemeshow, S. 2000. *Applied logistic regression*, second edition. John Wiley and Sons, New York, New York, USA
- Kendall, W.L., Hines, J.E., Nichols, J.D., and Grant, E.H.C. 2013. Relaxing the closure assumption in occupancy models: staggered arrival and departure times. *Ecology* 94: 610-617.

- Kjar, D., and Barrows, E.M. 2004. Arthropod community heterogeneity in a Mid-Atlantic forest highly invaded by alien organisms. *Banisteria* 24:26-37.
- Krauss, J., Steffan-Dewenter, I. and Tschardtke, T. 2003. How does landscape context contribute to effects of habitat fragmentation on diversity and population density of butterflies? *Journal of Biogeography* 30:889-900.
- Kuefler, D., Hudgens, B., Haddad, N.M., Morris, W.F., and Thurgate, N. 2010. The conflicting role of matrix habitats as conduits and barriers for dispersal. *Ecology* 91:944-950.
- Laurance, W.F. 2008. Theory meets reality: how habitat fragmentation research has transcended island biogeographic theory. *Biological Conservation* 141:1731-1744.
- Lederhouse, R.C. 1982. Factors affecting equal catchability in two swallowtail butterflies, *Papilio polyxenes* and *P. glaucus*. *Ecological Entomology* 7:379-383.
- Leu, M., Hanser, S.E., Aldridge, C.L., Cade, B.S. and Knick, S.T. 2011 A sampling and analytical approach to develop spatial distribution models for sagebrush-associated species. Pages 387–409 in *Sagebrush ecosystem conservation and management: Ecoregional assessment tools and models for the Wyoming Basins*. S.E. Hanser, M. Leu, S.T. Knick and C.L. Aldridge (editors). Allen Press, Lawrence, Kansas, USA.
- MacKenzie, D.I., Nichols, J.D., Hines, J.E., Knutson, M.G., and Franklin, A.B. 2003. Estimating site occupancy, colonization, and local extinction when a species is detected imperfectly. *Ecology* 84:2200-2207.

- MacKenzie, D.I., J.D. Nichols, J.A. Royle, K.H. Pollock, L.L. Bailey, and J.E. Hines. 2006. Occupancy estimation and modeling: inferring patterns and dynamics of species occurrence. Academic Press, Burlington, Massachusetts, USA.
- Matteson, K.C., Grace, J.B., and Minor, E.S. 2013. Direct and indirect effects of land use on floral resources and flower-visiting insects across an urban landscape. *Oikos* 122:682-694.
- Monette, R., and Ware, S. 1983. Early forest succession in the Virginia Coastal Plain. *Bulletin of the Torrey Botanical Club* 110:80–86.
- Morsdorf, F., Kötz, B., Meier, E., Itten, K. I., and Allgöwer, B. 2006. Estimation of LAI and fractional cover from small footprint airborne laser scanning data based on gap fraction. *Remote Sensing of Environment* 104:50–61.
- Opler, P.A., and Krizek, G.O. 1984. Butterflies east of the Great Plains: An illustrated natural history. Johns Hopkins University Press, Baltimore, Maryland, USA.
- Parks, C.R., Wendel, J.F., Sewell, M.M., Qiu, Y.L. 1994. The significance of allozyme variation and introgression in the *Liriodendron tulipifera* complex Magnoliaceae. *American Journal Botany* 81:878-889.
- Parmesan, C., Burrows, M.T., Duarte, C.M., Poloczanska, E.S., Richardson, A.J., Schoeman, D.S. and Singer, M.C. 2013. Beyond climate change attribution in conservation and ecological research. *Ecology letters* 16:58-71.
- Pellet, J. 2008. Season variation in detectability of butterflies surveyed with Pollard walks. *Journal of Insect Conservation* 12:155–162.

- Pollard, E. and T.J. Yates. 1993. Monitoring butterflies for ecology and conservation. Chapman and Hall, London, United Kingdom.
- R Core Team. 2013. R: a language and environment for statistical computing. R Foundation for Statistical Computing, Vienna, Austria. <http://www.R-project.org>.
- Radchuk, V., Turlure, C. and Schtickzelle, N. 2013. Each life stage matters: the importance of assessing the response to climate change over the complete life cycle in butterflies. *Journal of Animal Ecology* 82:275-285.
- Ries, L., Debinski, D.M. and Wieland, M.L. 2001. Conservation value of roadside prairie restoration to butterfly communities. *Conservation Biology* 15:401-411.
- Ries, L. and Sisk, T.D. 2008. Butterfly edge effects are predicted by a simple model in a complex landscape. *Oecologia* 156:75-86.
- Ries, L. and Sisk, T.D., 2010. What is an edge species? The implications of sensitivity to habitat edges. *Oikos* 119:1636-1642.
- Rooney, T.P. 2009. High white-tailed deer densities benefit graminoids and contribute to biotic homogenization of forest ground-layer vegetation. *Plant Ecology* 202:103-111.
- Roth, T., Strebel, N., and Amrhein, V. 2014. Estimating unbiased phenological trends by adapting site–occupancy models. *Ecology* 95:2144–2154.
- Saunders, D.A., Hobbs, R.J., and Margules, C.R. 1991. Biological consequences of ecosystem fragmentation: a review. *Conservation Biology* 5:18-32.

- Scriber, J.M., 1986. Origins of the regional feeding abilities in the tiger swallowtail butterfly: ecological monophagy and the *Papilio glaucus australis* subspecies in Florida. *Oecologia* 71:94-103.
- Schultz, C.B. and Crone, E.E. 2001. Edge-mediated dispersal behavior in a prairie butterfly. *Ecology* 82:1879–1892.
- Schultz, C.B. and Dlugosch, K. 1999. Nectar and host plant scarcity limit populations of an endangered Oregon butterfly. *Oecologia* 119:231–238.
- Scott, J.A. 1974. Mate-locating behavior of butterflies. *American Midland Naturalist* 91:103-117.
- Scott, J.A. 1975. Flight patterns among eleven species of diurnal Lepidoptera. *Ecology* 56: 1367-1377.
- Scott, J.A. 1992. The butterflies of North America: a natural history and field guide. Stanford University Press, Stanford, California, USA.
- Staudt, A., Leidner, A.K., Howard, J., Brauman, K.A., Dukes, J.S., Hansen, L.J., Paukert, C., Sabo, J. and Solórzano, L.A. 2013. The added complications of climate change: understanding and managing biodiversity and ecosystems. *Frontiers in Ecology and the Environment* 11:494-501.
- Sullivan, J. 1993. *Asimina triloba*. In: Fire Effects Information System, [Online]. U.S. Department of Agriculture, Forest Service, Rocky Mountain Research Station, Fire Sciences Laboratory Producer. www.fs.fed.us/database/feis, (accessed 8/11/2015).
- Tallamy, D.W., and Shropshire, K.J. 2009. Ranking Lepidopteran use of native versus introduced plants. *Conservation Biology* 23:941-947.

- Tewksbury, J.J., Levey, D.J., Haddad, N.M., Sargent, S., Orrock, J.L., Weldon, A., and Townsend, P. 2002. Corridors affect plants, animals, and their interactions in fragmented landscapes. *Proceedings of the National Academy of Sciences* 99:12923-12926.
- Thomas, C.D., Singer, M.C., and Boughton, D.A. 1996. Catastrophic extinction of population sources in a butterfly metapopulation. *The American Naturalist* 148:957-975.
- Thomas, J.A., Bourn, N.A.D., Clarke, R.T., Stewart, K.E., Simcox, D.J., Pearman, G.S., Curtis, R. and Goodger, B. 2001. The quality and isolation of habitat patches both determine where butterflies persist in fragmented landscapes. *Proceedings of the Royal Society of London B: Biological Sciences* 268:1791-1796.
- Tobin, E.J., Visser, J.M., Peterson, J.K. and Leberg, P.L. 2014. Small-mammal occupancy in freshwater marshes of Mandalay National Wildlife Refuge, Louisiana. *Southeastern Naturalist* 13:463-474.
- van Strien, A.J., C.A.M. van Swaay, and Kéry, M. 2011. Metapopulation dynamics in the butterfly *Hipparchia semele* changed decades before occupancy declined in the Netherlands. *Ecological Applications* 21:2510–2520.
- Vierling, K.T., Vierling, L.A., Gould, W.A., Martinuzzi, S., and Clawges, R.M. 2008. Lidar: shedding new light on habitat characterization and modeling. *Frontiers in Ecology and the Environment* 6:90–98.
- Wagner, D.L. 2005. *Caterpillars of eastern North America: a guide to identification and natural history*. Princeton University Press, Princeton, New Jersey, USA.

Wilcove, D.S., Rothstein, D., Dubow, J., Phillips, A., and Losos, E. 1998. Quantifying threats to imperiled species in the United States. *BioScience* 48:607–615.

Willson, M.F., and Schemske, D.W. 1980. Pollinator limitation, fruit production, and floral display in pawpaw (*Asimina triloba*). *Bulletin of the Torrey Botanical Club* 107:401-408.

Table 1: Variables measured in the field or derived from discrete-return light detection and ranging (LiDAR) data within 90 m buffers surrounding each transect, and land cover data derived from LANDFIRE Existing Vegetation Type (www.landfire.gov) within 270 m, 540 m, 1 km, 3 km, and 5 km buffers surrounding each transect for *Papilo glaucus* (PAGL) and *Euridydes marcellus* (EUMA).

Extent	Variable	Parameter estimated
90 m (measured on the transect or from LiDAR data)	Basal area of deciduous canopy	Occupancy
	Number of deciduous trees in the canopy	Occupancy
	Basal area of potential hostplants for <i>P. glaucus</i> in the canopy	Occupancy (PAGL only)
	Count <i>P. glaucus</i> host plant understory	Occupancy (PAGL only)
	Count <i>P. glaucus</i> host plant canopy	Occupancy (PAGL only)
	Count <i>P. glaucus</i> host plant sub-canopy	Occupancy (PAGL only)
	Proportion <i>A. triloba</i>	Occupancy (EUMA only)
	Nectar score	Detection probability, Colonization, Extinction
	Wind (m/s)	Detection probability
	Temperature (°C)	Detection probability
	Season	Detection probability
	Sampling occasion	Detection probability
	Structural heterogeneity of vegetation 0.3-3.0 m above ground	Colonization (PAGL) Extinction (EUMA)
	Structural heterogeneity > 3 m above ground	Colonization
270 m, 540 m, 1 km, 3 km, 5 km (derived from LANDFIRE EVT)	Proportion agriculture	Colonization
	Proportion open herbaceous	Colonization
	Proportion early successional	Colonization
	Proportion riparian	Colonization
	Density of edges between forest and	Colonization

agriculture	
Edge density forest-open herbaceous	Colonization
Density of local roads	Colonization
Density of other roads	Colonization
Proportion wetland	Extinction
Basal area coniferous canopy	Extinction
Count coniferous canopy	Extinction
Proportion canopy	Extinction
Edge mixed/deciduous wetlands	Extinction
Edge forest wetlands	Extinction
Proportion floodplain	Colonization (PAGL) Extinction (EUMA)
Proportion upland	Colonization (PAGL) Extinction (EUMA)

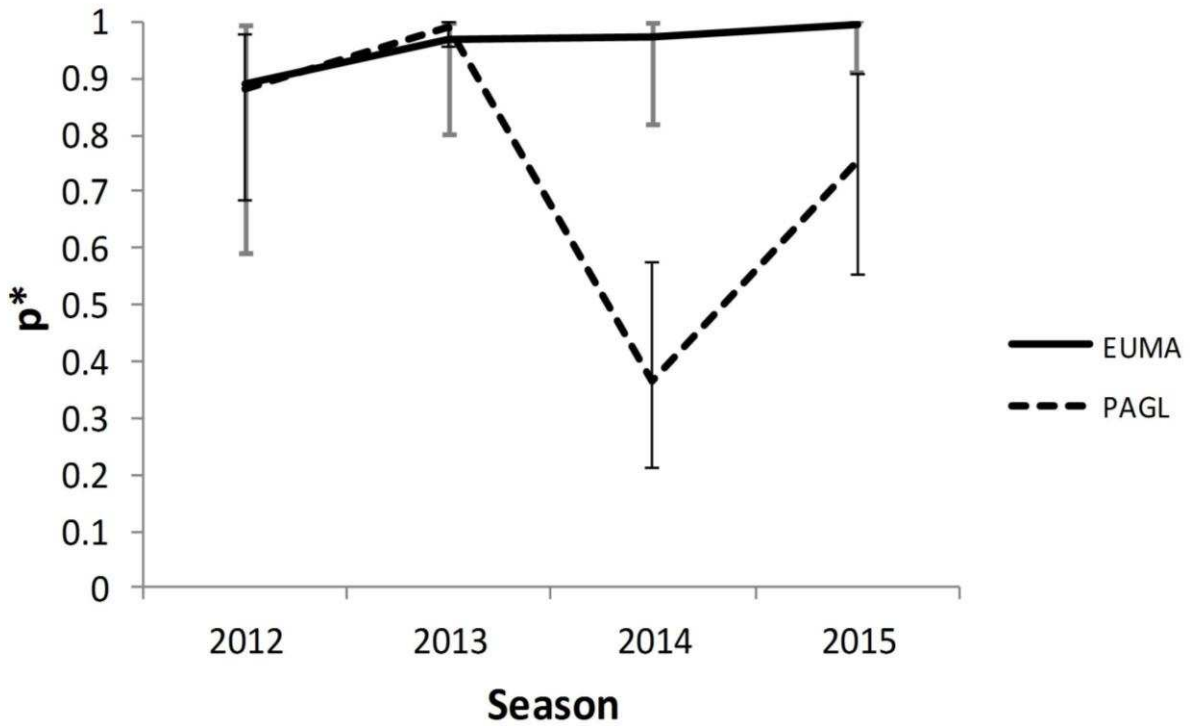


Figure. 1: Probability (\pm 95% confidence interval) of detecting *Eurytides marcellus* (EUMA) and *Papilio glaucus* (PAGL) at least once during each season (p^*). P^* was nearly constant across seasons for *E. marcellus* but varied greatly among seasons for *P. glaucus*, with p^* decreasing to < 0.5 in 2014. Estimates for *E. marcellus* were based on a model of occupancy that included the interaction of season and occasion ($\psi [.] \gamma [.] \varepsilon [.] e [.] d [.] p [\text{season} * \text{survey}]$) model. Estimates for *P. glaucus* were also based on a model of occupancy that included an additive model of season and survey ($\psi [.] \gamma [.] \varepsilon [.] e [.] d [.] p [\text{season} + \text{survey}]$) model.

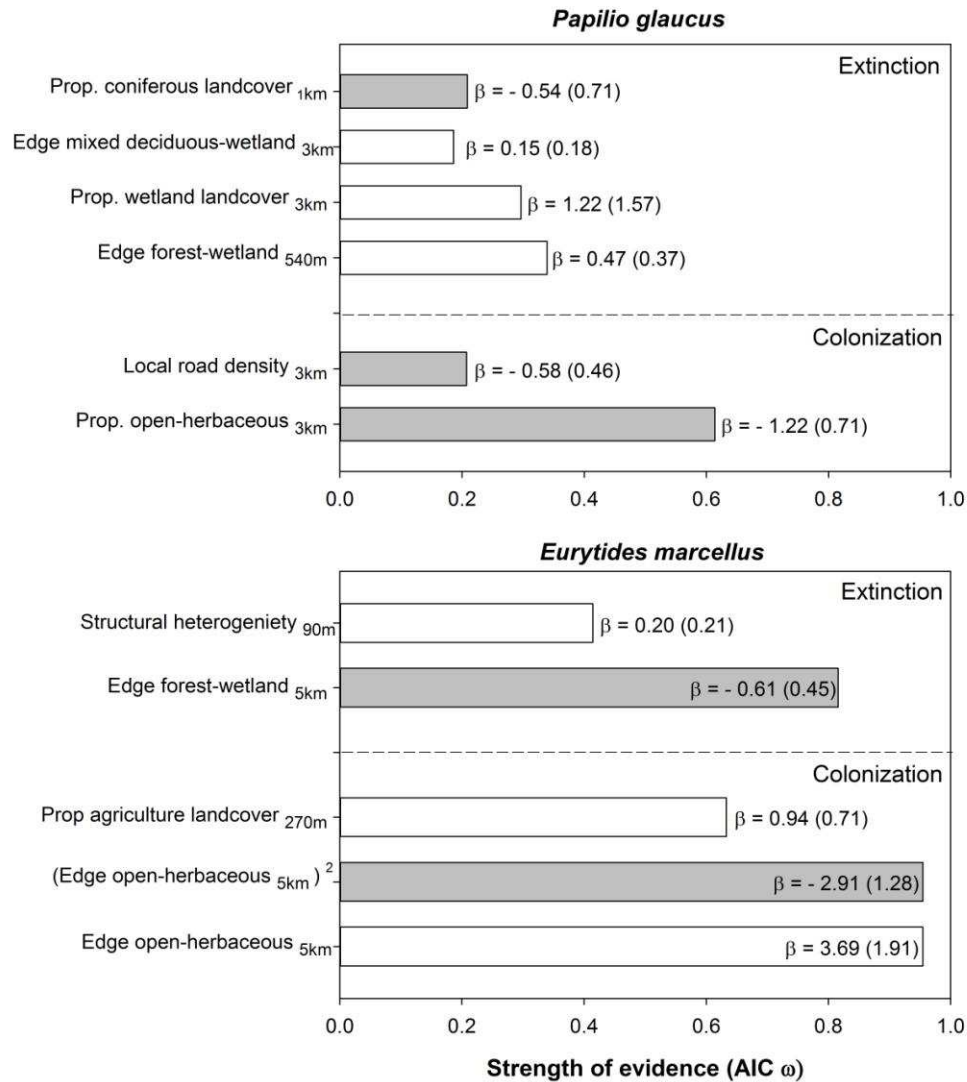


Figure 2: Summed AIC model weights, conditional model-averaged regression coefficients (β) and unconditional standard errors (SE) for variables included in the most strongly supported multivariate models of colonization and extinction for *Papilio glaucus* and *Eurytides marcellus*. Intercepts for *Papilio glaucus*: INTcolonization ($\beta = -0.62 \pm 1.66$), INTeffectsize ($\beta = 3.33 \pm 1.85$), INTextinction ($\beta = -2.85 \pm 1.30$), INTeffectsize ($\beta = -0.67 \pm 2.82$), INTeffectsize 2013-2014 ($\beta = -0.17 \pm 0.7$), INTeffectsize 2014-2015 ($\beta =$

0.76 ± 0.76). Intercepts for *Eurytides marcellus*: INTcolonization 2012-2013 ($\beta = -0.58 \pm 1.39$), INTcolonization 2013-2014 ($\beta = -3.64 \pm 3.83$), INTcolonization 2014-2015 ($\beta = 0.58 \pm 1.20$), INTextinction 2012-2013 ($\beta = -2.61 \pm 0.90$), INTextinction 2013-2014 ($\beta = -1.72 \pm 0.64$), INTextinction 2014-2015 ($\beta = -2.54 \pm 0.97$).

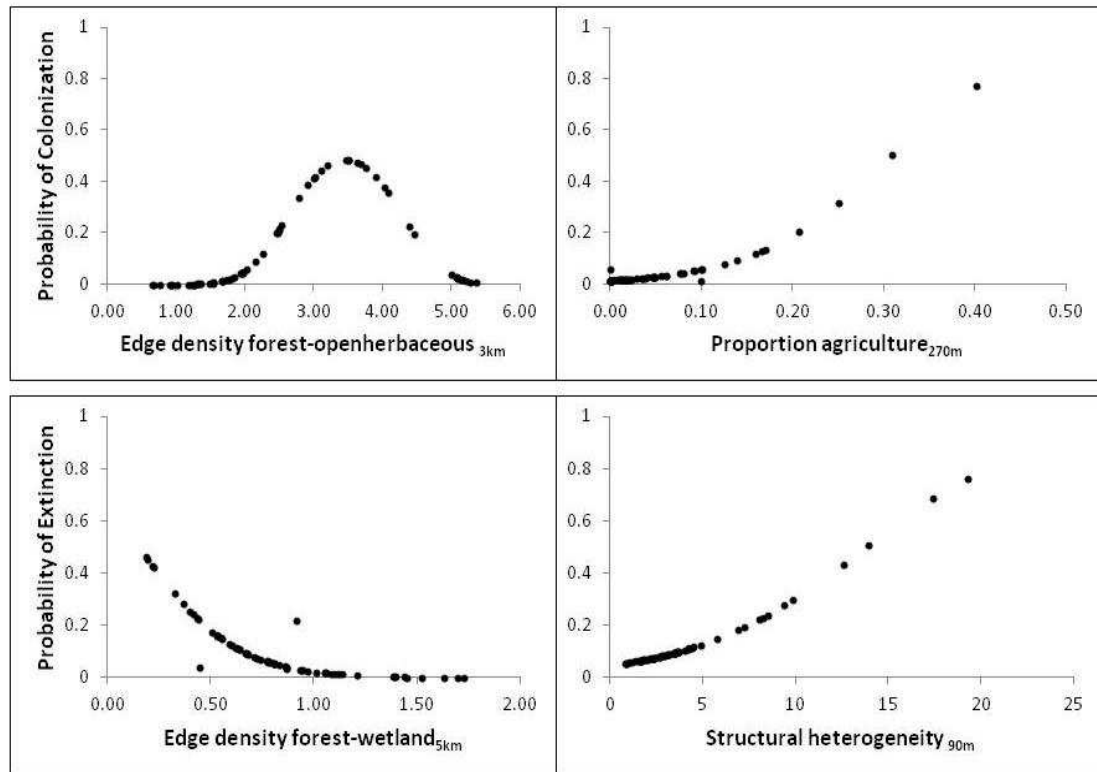


Figure 3: Associations between independent variables that were in the set of most strongly supported models and probability of extinction or colonization for *Eurytides marcellus*.

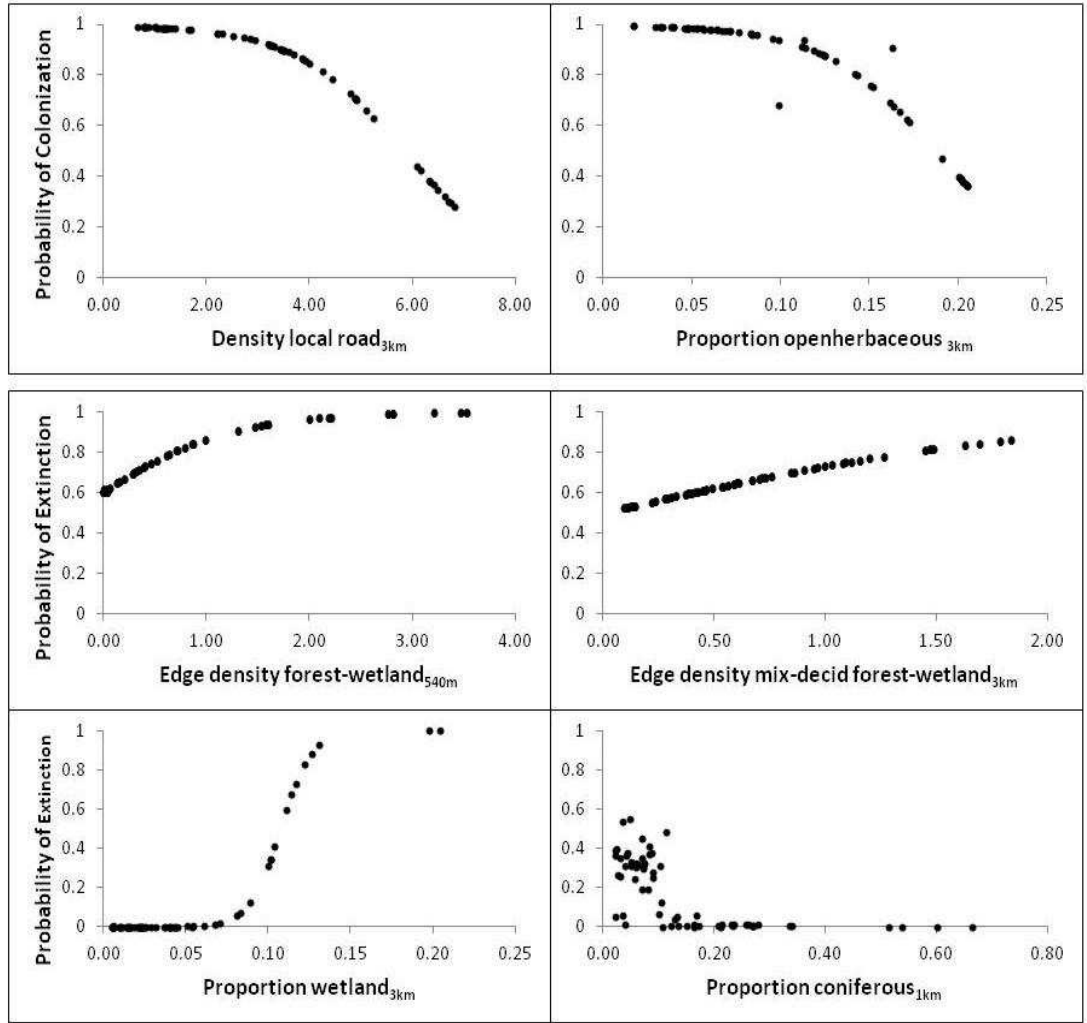


Figure 4: Associations between independent variables that were in the set of most strongly supported models and probability of extinction or colonization for *Papilio glaucus*.

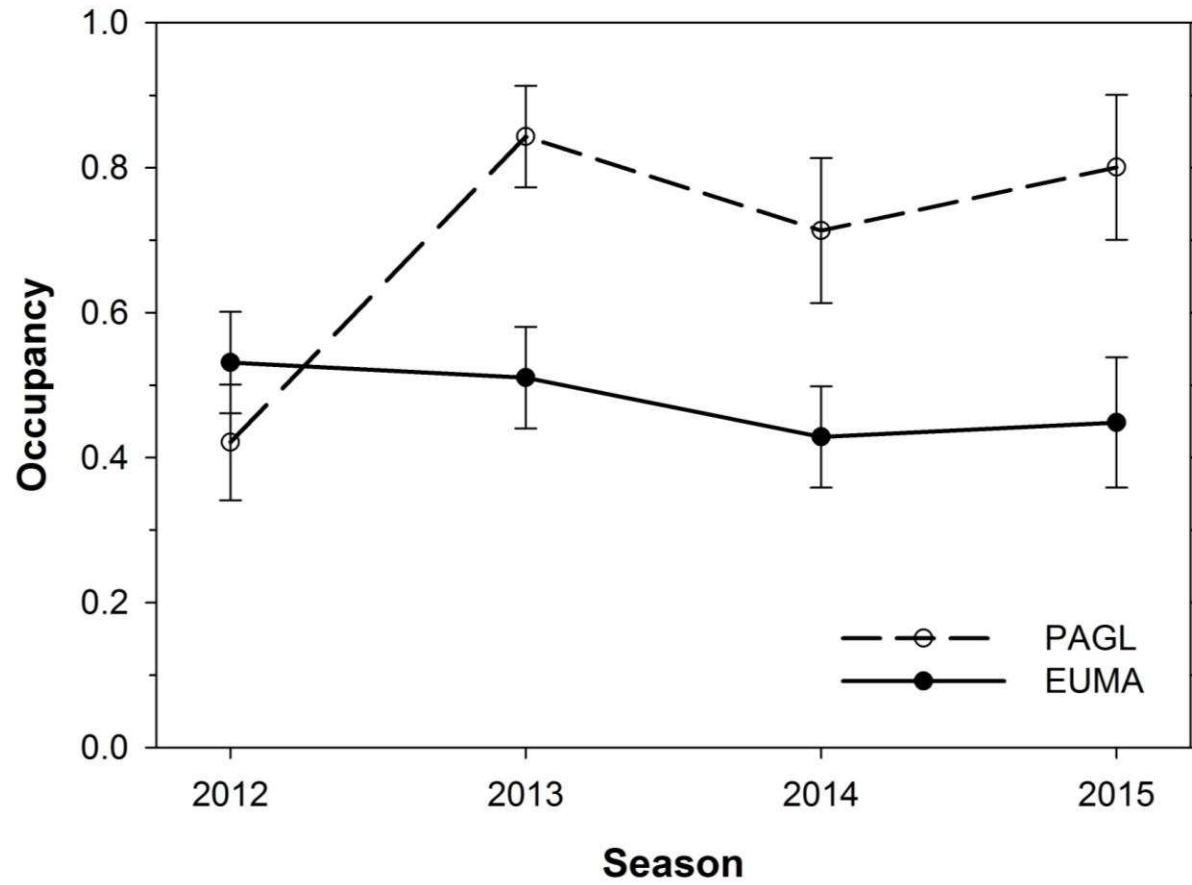


Figure 5: Probability (\pm SE) of occupancy of *Eurytides marcellus* (EUMA) and *Papilio glaucus* (PAGL) across four seasons (2012-2015). Occupancy for *E. marcellus* was relatively stable whereas it increased nearly twofold in 2013 for *P. glaucus*. Estimates for *E.*

marcellus were based on the (ψ [.] γ [season] ε [season] e [.] d [.] p [season*survey]) model. Estimates for *P. glaucus* were based on the (ψ [.] γ [season] ε [season] e [.] d [.] p [season + survey]) model.

APPENDICES

Appendix 1: LANDFIRE Existing Vegetation Types (www.landfire.gov) included within each land-cover class in models of occupancy of *Papilio glaucus* and *Eurytides marcellus*.

Land-cover class	Existing vegetation types
Agriculture	61, 62, 63, 64, 65, 82
Open herbaceous	16, 17, 67, 81, 2181, 2531, 2545
Wetland	75, 76, 95, 2185, 2436, 2452
Riparian	2472, 2474
Upland mixed	13, 15, 2324, 2368, 2370, 2400
Mesic mixed	2303, 2316, 2335, 2343
Coniferous	14, 2347, 2456, 2534, 2535, 2542
Early successional	2191, 2532, 2533, 2541, 2543
Floodplain	2471, 2473
Mixed deciduous forest	13, 15, 2324, 2368, 2370, 2400, 2303, 2316, 2335, 2343
Mixed deciduous/coniferous forest	13, 15, 2324, 2368, 2370, 2400, 2303, 2316, 2335, 2343, 14, 2347, 2456, 2534, 2535, 2542

Appendix 2: Strengths of support for open and closed multi-season occupancy models for *Eurytides marcellus* and *Papilio glaucus*.

Psi = occupancy, p = detection, gam = colonization, eps = extinction, e = entry, d = departure, AICc = Akaike's Information Criterion adjusted for small sample size, ΔAIC = difference from the model with the lowest AIC, and $AIC\omega$ = model weight.

Species	Model	AIC _c	ΔAIC	AIC ω	Number of parameters
<i>Eurytides marcellus</i>	psi(.),gam(.),eps(.),e(.),d(.),p(.)	1126.22	0.00	0.99	6
	psi(.),gamma(.),eps(.),p(.)	1136.31	10.09	0.01	4
<i>Papilio glaucus</i>	psi(.),gam(.),eps(.),e(.),d(.),p(.)	1315.16	0.00	1.00	6
	psi(.),gamma(.),eps(.),p(.)	1332.80	17.64	0.00	4

Appendix 3: Strengths of support for models of the detection probability of *Eurytides marcellus*. Psi = occupancy, p = detection, gam = colonization, eps = extinction, e = entry, and d = departure, full id = season*survey interaction, survey[int_p6] = survey 6 set as intercept, Q = quadratic function ($x + x^2$), T = a pseudo-threshold function ($\ln[x]$), rain = days since rain, rainQ = quadratic function of days since rain, temp = linear function of temperature ($^{\circ}\text{C}$), tempQ = quadratic function of temperature, wind = wind speed (m/s), windQ = quadratic function of wind speed, nectar = abundance of nectar where the high abundance class is the intercept. AICc = Akaike's Information Criterion adjusted for small sample size, ΔAIC = AIC difference value, and $\text{AIC}\omega$ = AIC model weight.

Model	AICc	ΔAIC	$\text{AIC}\omega$	Model Likelihood	Number of parameters
psi(.),gam(.),eps(.),e(.),d(.),p(full_id_rain)	1081.92	0.00	0.52	1.00	30
psi(.),gam(.),eps(.),e(.),d(.),p(full_id_rainQ)	1083.36	1.44	0.25	0.49	31
psi(.),gam(.),eps(.),e(.),d(.),p(full_id_temp)	1085.48	3.56	0.08	0.17	30
psi(.),gam(.),eps(.),e(.),d(.),p(full_id)	1086.87	4.95	0.04	0.08	29
psi(.),gam(.),eps(.),e(.),d(.),p(full_id_tempQ)	1087.45	5.53	0.03	0.06	31
psi(.),gam(.),eps(.),e(.),d(.),p(full_id_nectar high)	1088.72	6.80	0.02	0.03	30
psi(.),gam(.),eps(.),e(.),d(.),p(full_id_nectar low)	1088.78	6.86	0.02	0.03	30
psi(.),gam(.),eps(.),e(.),d(.),p(full_id_wind)	1088.88	6.96	0.02	0.03	30
psi(.),gam(.),eps(.),e(.),d(.),p(full_id_windQ)	1090.47	8.55	<0.01	0.01	31
psi(.),gam(.),eps(.),e(.),d(.),p(season+survey[int_p6])	1101.16	19.24	<0.01	<0.01	14
psi(.),gam(.),eps(.),e(.),d(.),p(season+survey[int_p6]+wind)	1104.24	22.32	<0.01	<0.01	15
psi(.),gam(.),eps(.),e(.),d(.),p(survey)	1113.61	31.69	<0.01	<0.01	11
psi(.),gam(.),eps(.),e(.),d(.),p(season)	1117.95	36.03	<0.01	<0.01	9
psi(.),gam(.),eps(.),e(.),d(.),p(.)	1126.19	44.27	<0.01	<0.01	6

psi(.),gamma(.),eps(.),p(.)	1136.28	54.36	<0.01	<0.01	4
-----------------------------	---------	-------	-------	-------	---

Appendix 4: Strengths of support for models of the detection probability for *Papilio glaucus*. Psi = occupancy, p = detection, gam = colonization, eps = extinction, e = entry, and d = departure, full id = season*survey interaction, survey[int_p6] = survey 6 set as intercept, Q = quadratic function ($x + x^2$), T = a pseudo-threshold function ($\ln[x]$)rain = days since rain, rainQ = quadratic function of days since rain, temp = linear function of temperature ($^{\circ}\text{C}$), tempQ = quadratic function of temperature, wind = wind speed (m/s), windQ = quadratic function of wind speed, nectar = abundance of nectar where the high abundance class is the intercept. AICc = Akaike's Information Criterion adjusted for small sample size, ΔAIC = AIC difference value, and $\text{AIC}\omega$ = AIC model weight.

Model	AIC	ΔAIC	$\text{AIC}\omega$	Model Likelihood	Number of parameters
psi(.),gam(.),eps(.),e(.),d(.),p(season+survey[int_p6])+nectar)	1177.49	0.00	0.98	1.00	15
psi(.),gam(.),eps(.),e(.),d(.),p(season+survey[int_p6])	1188.77	11.28	<0.01	<0.01	14
psi(.),gam(.),eps(.),e(.),d(.),p(season+survey[int_p6]+rain)	1188.90	11.41	<0.01	<0.01	15
psi(.),gam(.),eps(.),e(.),d(.),p(season+survey[int_p6]+temp)	1189.09	11.60	<0.01	<0.01	15
psi(.),gam(.),eps(.),e(.),d(.),p(season+survey[int_p6]+wind)	1189.09	11.60	<0.01	<0.01	15
psi(.),gam(.),eps(.),e(.),d(.),p(season+survey[int_p6]+windQ)	1189.57	12.08	<0.01	<0.01	16
psi(.),gam(.),eps(.),e(.),d(.),p(season+survey[int_p6]+rainQ)	1189.98	12.49	<0.01	<0.01	16
psi(.),gam(.),eps(.),e(.),d(.),p(season+survey[int_p6]+tempQ)	1190.96	13.47	<0.01	<0.01	16
psi(.),gam(.),eps(.),e(.),d(.),p(fullid)	1194.56	17.07	<0.01	<0.01	29
psi(.),gam(.),eps(.),e(.),d(.),p(season+survey +rainQ)	1207.16	29.67	<0.01	<0.01	19
psi(.),gam(.),eps(.),e(.),d(.),p(season+survey +nectar)	1208.23	30.74	<0.01	<0.01	14
psi(.),gam(.),eps(.),e(.),d(.),p(season+survey +tempQ)	1228.20	50.71	<0.01	<0.01	19
psi(.),gam(.),eps(.),e(.),d(.),p(season+survey +wind)	1234.09	56.60	<0.01	<0.01	14
psi(.),gam(.),eps(.),e(.),d(.),p(season+survey +windQ)	1234.16	56.67	<0.01	<0.01	19

psi(.),gam(.),eps(.),e(.),d(.),p(season+survey +rain)	1234.52	57.03	<0.01	<0.01	14
psi(.),gam(.),eps(.),e(.),d(.),p(season+survey +temp)	1234.57	57.08	<0.01	<0.01	14
psi(.),gam(.),eps(.),e(.),d(.),p(.)	1314.78	137.29	<0.01	<0.01	6

Appendix 5: Strengths of support for univariate models of occupancy of *Eurytides marcellus* while keeping the best detection model constant. Psi = occupancy, p = detection, gam = colonization, eps = extinction, e = entry, and d = departure, full_id = season*survey interaction, rain= days since rain, Q = quadratic function ($x + x^2$), T = a pseudo-threshold function ($\ln[x]$), prop_paw = proportion meter intervals intercepted by *A. triloba*, prop_pawT = pseudo-threshold function of proportion meter intervals intercepted by *A. triloba*, prop_pawQ = quadratic function of proportion *A. triloba*, basal_decid_canopy = the basal area of deciduous canopy trees, basal_decid_canopyT = the pseudo-threshold function basal area of deciduous canopy trees, basal_decid_canopy Q= the quadratic function of basal area of deciduous canopy trees and AIC = Akaike's Information Criterion adjusted for sample size, ΔAIC = difference from the top model AIC, and AIC_{ω} = model weight.

Model	AIC	ΔAIC	AIC_{ω}	Model Likelihood	Number of parameters
psi(prop_pawT),gam(.),eps(.),e(.),d(.),p(full_id + rain)	1071.79	0.00	0.42	1.00	31
psi(prop_paw),gam(.),eps(.),e(.),d(.),p(full_id + rain)	1071.84	0.05	0.41	0.98	31
psi(prop_pawQ),gam(.),eps(.),e(.),d(.),p(full_id + rain)	1073.80	2.01	0.15	0.37	32
psi(.),gam(.),eps(.),e(.),d(.),p(full_id + rain)	1081.92	10.13	<0.01	<0.01	30
psi(basal_decid_can),gam(.),eps(.),e(.),d(.),p(full_id + rain)	1082.71	10.92	<0.01	<0.01	31
psi(basal_decid_canT),gam(.),eps(.),e(.),d(.),p(full_id + rain)	1082.88	11.09	<0.01	<0.01	31
psi(basal_decid_canQ),gam(.),eps(.),e(.),d(.),p(full_id + rain)	1082.99	11.20	<0.01	<0.01	32

Appendix 6: Strengths of support for univariate models of occupancy of *Papilio glaucus* while keeping the best detection probability model constant. Psi = occupancy, p = detection, gam = colonization, eps = extinction, e = entry, and d = departure, survey[int_p6] = survey 6 set as intercept, rain = days since rain, Q = quadratic function ($x + x^2$), T = a pseudo-threshold function ($\ln[x]$), basal_decid_canopy = the basal area of deciduous trees in the canopy, count_host_us = number of potential host plants for *P. glaucus* in the understory, count_host_sc = number of potential host plants for *P. glaucus* in the subcanopy, count_host_canopy = number of potential host plants for *P. glaucus* in the canopy, AICc = Akaike's Information Criterion adjusted for small sample size, ΔAIC = difference from the top model AIC, and AIC ω = model weight.

Model	AICc	ΔAIC	AIC ω	Model Likelihood	Number of parameters
psi(count_host_usT),gam(.),eps(.),e(.),d(.),p(season+survey[int_p6])	1187.16	0.00	0.18	1.00	15
psi(count_host_us),gam(.),eps(.),e(.),d(.),p(season+survey[int_p6])	1187.18	0.02	0.18	0.99	15
psi(count_host_usQ),gam(.),eps(.),e(.),d(.),p(season+survey[int_p6])	1187.78	0.62	0.14	0.73	15
psi,gam(.),eps(.),e(.),d(.),p(season+survey [int_p6])	1188.77	1.61	0.08	0.45	14
psi(basal_host_canopyT),gam(.),eps(.),e(.),d(.),p(season+survey[int_p6])	1190.06	2.90	0.04	0.23	15
psi(count_host_canopyQ),gam(.),eps(.),e(.),d(.),p(season+survey[int_p6])	1190.15	2.99	0.04	0.22	15
psi(count_host_canopy),gam(.),eps(.),e(.),d(.),p(season+survey[int_p6])	1190.42	3.26	0.04	0.20	15
psi(count_host_canopyT),gam(.),eps(.),e(.),d(.),p(season+survey[int_p6])	1190.48	3.32	0.04	0.19	15
psi(basal_host_canopy),gam(.),eps(.),e(.),d(.),p(season+survey[int_p6])	1190.50	3.34	0.03	0.19	15
psi(basal_decid_canopyQ),gam(.),eps(.),e(.),d(.),p(season+survey[int_p6])	1190.52	3.36	0.03	0.19	15
psi(count_host_subcanopyQ),gam(.),eps(.),e(.),d(.),p(season+survey[int_p6])	1190.60	3.44	0.03	0.18	15
psi(basal_decid_canopyT),gam(.),eps(.),e(.),d(.),p(season+survey[int_p6])	1190.62	3.46	0.03	0.18	15

psi(basal_host_canopyQ),gam(.),eps(.),e(.),d(.),p(season+survey[int_p6])	1190.71	3.55	0.03	0.17	15
psi(count_host_subcanopy),gam(.),eps(.),e(.),d(.),p(season+survey[int_p6])	1190.71	3.55	0.03	0.17	15
psi(count_host_subcanopyT),gam(.),eps(.),e(.),d(.),p(season+survey[int_p6])	1190.74	3.58	0.03	0.17	15
psi(basal_decid_canopy),gam(.),eps(.),e(.),d(.),p(season+survey[int_p6])	1190.75	3.59	0.03	0.17	15

Appendix 7: Strengths of support for univariate models of colonization of *E. marcellus* while keeping the best detection probability model constant. Psi = occupancy, p = detection, gam = colonization, eps = extinction, e = entry, and d = departure, full_id = season*survey interaction, rain = days since rain, Q = quadratic function ($x + x^2$), T = a pseudo-threshold function ($\ln[x]$), edge_foroh = edge density forest-open herbaceous, prop_ag = proportion agriculture, prop_succ = proportion successional, edge_forag = edge density forest-agriculture, prop_rip = proportion riparian, prop_mesic = proportion mesic, road_other = other roads, road_local = local roads, prop_oh = proportion open herbaceous , and AIC = Akaike's Information Criterion adjusted for sample size, ΔAIC = difference from the top model AIC, and $AIC\omega$ = model weight.

Model	AIC	ΔAIC	$AIC\omega$	Model Likelihood	Number of parameters
psi(.),gam(edge_foroh_3kmQ+year),eps(.),e(.),d(.),p(full_id+rain)	1079.34	0.00	0.11	1.00	34
psi(.),gam(prop_ag_270m+year),eps(.),e(.),d(.),p(full_id+rain)	1080.68	1.34	0.06	0.51	33
psi(.),gam(prop_ag_270mT+year),eps(.),e(.),d(.),p(full_id+rain)	1080.94	1.60	0.05	0.45	33
psi(.),gam(prop_succ_3kmQ+year),eps(.),e(.),d(.),p(full_id+rain)	1081.44	2.10	0.04	0.35	34
psi(.),gam(.),eps(.),e(.),d(.),p(full_id+rain)	1081.92	2.58	0.03	0.28	30
psi(.),gam(prop_ag_270mQ+year),eps(.),e(.),d(.),p(full_id+rain)	1082.06	2.72	0.03	0.26	34
psi(.),gam(prop_ag_1kmQ+year),eps(.),e(.),d(.),p(full_id+rain)	1082.18	2.84	0.03	0.24	34
psi(.),gam(edge_forag_270mT+year),eps(.),e(.),d(.),p(full_id+rain)	1082.44	3.10	0.02	0.21	33
psi(.),gam(prop_ag_1km+year),eps(.),e(.),d(.),p(full_id+rain)	1082.51	3.17	0.02	0.20	33
psi(.),gam(edge_forag_270m+year),eps(.),e(.),d(.),p(full_id+rain)	1082.80	3.46	0.02	0.18	33
psi(.),gam(road_other_3kmQ+year),eps(.),e(.),d(.),p(full_id+rain)	1082.88	3.54	0.02	0.17	34
psi(.),gam(road_other_540kmQ+year),eps(.),e(.),d(.),p(full_id+rain)	1082.94	3.60	0.02	0.17	34

psi(.),gam(road_other_540mQ+year),eps(.),e(.),d(.),p(full_id+rain)	1082.94	3.60	0.02	0.17	34
psi(.),gam(prop_ag_1kmT+year),eps(.),e(.),d(.),p(full_id+rain)	1083.01	3.67	0.02	0.17	33
psi(.),gam(prop_rip_540mQ+year),eps(.),e(.),d(.),p(full_id+rain)	1083.14	3.80	0.02	0.15	34
psi(.),gam(prop_rip_270mT+year),eps(.),e(.),d(.),p(full_id+rain)	1083.21	3.87	0.02	0.14	33
psi(.),gam(edge_forag_270mQ+year),eps(.),e(.),d(.),p(full_id+rain)	1083.21	3.87	0.02	0.14	34
psi(.),gam(prop_rip_270m+year),eps(.),e(.),d(.),p(full_id+rain)	1083.90	4.56	0.01	0.10	33
psi(.),gam(edge_forag_540mT+year),eps(.),e(.),d(.),p(full_id+rain)	1083.91	4.57	0.01	0.10	33
psi(.),gam(prop_mesic_270mT+year),eps(.),e(.),d(.),p(full_id+rain)	1083.96	4.62	0.01	0.10	33
psi(.),gam(prop_ag_540m+year),eps(.),e(.),d(.),p(full_id+rain)	1083.97	4.63	0.01	0.10	33
psi(.),gam(prop_ag_540mT+year),eps(.),e(.),d(.),p(full_id+rain)	1083.99	4.65	0.01	0.10	33
psi(.),gam(prop_rip_540m+year),eps(.),e(.),d(.),p(full_id+rain)	1084.18	4.84	< 0.01	0.09	33
psi(.),gam(prop_succ_5kmT+year),eps(.),e(.),d(.),p(full_id+rain)	1084.19	4.85	< 0.01	0.09	33
psi(.),gam(prop_pawpawQ+year),eps(.),e(.),d(.),p(full_id+rain)	1084.20	4.86	< 0.01	0.09	34
psi(.),gam(edge_forag_540mQ+year),eps(.),e(.),d(.),p(full_id+rain)	1084.28	4.94	< 0.01	0.08	34
psi(.),gam(prop_mesic_270m+year),eps(.),e(.),d(.),p(full_id+rain)	1084.29	4.95	< 0.01	0.08	33
psi(.),gam(prop_mesic_540mT+year),eps(.),e(.),d(.),p(full_id+rain)	1084.36	5.02	< 0.01	0.08	33
psi(.),gam(road_other_1kmQ+year),eps(.),e(.),d(.),p(full_id+rain)	1084.36	5.02	< 0.01	0.08	34
psi(.),gam(edge_forag_540m+year),eps(.),e(.),d(.),p(full_id+rain)	1084.42	5.08	< 0.01	0.08	33
psi(.),gam(road_local_3kmQ+year),eps(.),e(.),d(.),p(full_id+rain)	1084.66	5.32	< 0.01	0.07	34
psi(.),gam(edge_forag_1kmT+year),eps(.),e(.),d(.),p(full_id+rain)	1084.79	5.45	< 0.01	0.07	33
psi(.),gam(prop_succ_540mT+year),eps(.),e(.),d(.),p(full_id+rain)	1084.88	5.54	< 0.01	0.06	33
psi(.),gam(prop_ag_3km+year),eps(.),e(.),d(.),p(full_id+rain)	1084.90	5.56	< 0.01	0.06	33
psi(.),gam(prop_rip_540mT+year),eps(.),e(.),d(.),p(full_id+rain)	1084.90	5.56	< 0.01	0.06	33
psi(.),gam(prop_mesic_540m+year),eps(.),e(.),d(.),p(full_id+rain)	1084.92	5.58	< 0.01	0.06	33
psi(.),gam(edge_forag_1km+year),eps(.),e(.),d(.),p(full_id+rain)	1084.96	5.62	< 0.01	0.06	33
psi(.),gam(year),eps(.),e(.),d(.),p(full_id+rain)	1085.03	5.69	< 0.01	0.06	32

psi(.),gam(road_other_3km+year),eps(.),e(.),d(.),p(full_id+rain)	1085.03	5.69	< 0.01	0.06	33
psi(.),gam(prop_ag_5kmQ+year),eps(.),e(.),d(.),p(full_id+rain)	1085.27	5.93	< 0.01	0.05	34
psi(.),gam(prop_pawpawT+year),eps(.),e(.),d(.),p(full_id+rain)	1085.28	5.94	< 0.01	0.05	33
psi(.),gam(prop_rip_270mQ+year),eps(.),e(.),d(.),p(full_id+rain)	1085.29	5.95	< 0.01	0.05	34
psi(.),gam(prop_succ_5km+year),eps(.),e(.),d(.),p(full_id+rain)	1085.33	5.99	< 0.01	0.05	33
psi(.),gam(prop_ag_3kmT+year),eps(.),e(.),d(.),p(full_id+rain)	1085.41	6.07	< 0.01	0.05	33
psi(.),gam(prop_succ_1km+year),eps(.),e(.),d(.),p(full_id+rain)	1085.43	6.09	< 0.01	0.05	33
psi(.),gam(prop_succ_1kmT+year),eps(.),e(.),d(.),p(full_id+rain)	1085.54	6.20	< 0.01	0.05	33
psi(.),gam(road_other_3kmT+year),eps(.),e(.),d(.),p(full_id+rain)	1085.75	6.41	< 0.01	0.04	33
psi(.),gam(prop_rip_5kmQ+year),eps(.),e(.),d(.),p(full_id+rain)	1085.76	6.42	< 0.01	0.04	34
psi(.),gam(prop_rip_1km+year),eps(.),e(.),d(.),p(full_id+rain)	1085.83	6.49	< 0.01	0.04	33
psi(.),gam(prop_ag_540mQ+year),eps(.),e(.),d(.),p(full_id+rain)	1085.97	6.63	< 0.01	0.04	34
psi(.),gam(prop_rip_1kmT+year),eps(.),e(.),d(.),p(full_id+rain)	1086.01	6.67	< 0.01	0.04	33
psi(.),gam(prop_pawpaw+year),eps(.),e(.),d(.),p(full_id+rain)	1086.03	6.69	< 0.01	0.04	33
psi(.),gam(road_other_270mT+year),eps(.),e(.),d(.),p(full_id+rain)	1086.04	6.70	< 0.01	0.04	33
psi(.),gam(prop_succ_270mT+year),eps(.),e(.),d(.),p(full_id+rain)	1086.05	6.71	< 0.01	0.03	33
psi(.),gam(prop_oh_270m+year),eps(.),e(.),d(.),p(full_id+rain)	1086.07	6.73	< 0.01	0.03	33
psi(.),gam(prop_ag_3kmQ+year),eps(.),e(.),d(.),p(full_id+rain)	1086.09	6.75	< 0.01	0.03	34
psi(.),gam(edge_forag_3km+year),eps(.),e(.),d(.),p(full_id+rain)	1086.10	6.76	< 0.01	0.03	33
psi(.),gam(edge_forag_3kmT+year),eps(.),e(.),d(.),p(full_id+rain)	1086.12	6.78	< 0.01	0.03	33
psi(.),gam(prop_mesic_3kmQ+year),eps(.),e(.),d(.),p(full_id+rain)	1086.17	6.83	< 0.01	0.03	34
psi(.),gam(prop_mesic_270mQ+year),eps(.),e(.),d(.),p(full_id+rain)	1086.21	6.87	< 0.01	0.03	34
psi(.),gam(road_local_540m+year),eps(.),e(.),d(.),p(full_id+rain)	1086.24	6.90	< 0.01	0.03	33
psi(.),gam(edge_forag_1kmQ+year),eps(.),e(.),d(.),p(full_id+rain)	1086.32	6.98	< 0.01	0.03	34
psi(.),gam(prop_oh_270mT+year),eps(.),e(.),d(.),p(full_id+rain)	1086.32	6.98	< 0.01	0.03	33
psi(.),gam(road_local_270mT+year),eps(.),e(.),d(.),p(full_id+rain)	1086.35	7.01	< 0.01	0.03	33

psi(.),gam(roads_local_270m+year),eps(.),e(.),d(.),p(full_id+rain)	1086.35	7.01	< 0.01	0.03	33
psi(.),gam(prop_succ_3kmT+year),eps(.),e(.),d(.),p(full_id+rain)	1086.39	7.05	< 0.01	0.03	33
psi(.),gam(prop_succ_270m+year),eps(.),e(.),d(.),p(full_id+rain)	1086.43	7.09	< 0.01	0.03	33
psi(.),gam(prop_mesic_1km+year),eps(.),e(.),d(.),p(full_id+rain)	1086.43	7.09	< 0.01	0.03	33
psi(.),gam(prop_mesic_540mQ+year),eps(.),e(.),d(.),p(full_id+rain)	1086.49	7.15	< 0.01	0.03	34
psi(.),gam(road_local_540mT+year),eps(.),e(.),d(.),p(full_id+rain)	1086.55	7.21	< 0.01	0.03	33
psi(.),gam(prop_rip_3kmT+year),eps(.),e(.),d(.),p(full_id+rain)	1086.55	7.21	< 0.01	0.03	33
psi(.),gam(road_other_5kmT+year),eps(.),e(.),d(.),p(full_id+rain)	1086.58	7.24	< 0.01	0.03	33
psi(.),gam(prop_mesic_5kmT+year),eps(.),e(.),d(.),p(full_id+rain)	1086.61	7.27	< 0.01	0.03	33
psi(.),gam(prop_succ_540m+year),eps(.),e(.),d(.),p(full_id+rain)	1086.62	7.28	< 0.01	0.03	33
psi(.),gam(prop_mesic_1kmT+year),eps(.),e(.),d(.),p(full_id+rain)	1086.63	7.29	< 0.01	0.03	33
psi(.),gam(prop_ag_5km+year),eps(.),e(.),d(.),p(full_id+rain)	1086.63	7.29	< 0.01	0.03	33
psi(.),gam(prop_rip_3km+year),eps(.),e(.),d(.),p(full_id+rain)	1086.63	7.29	< 0.01	0.03	33
psi(.),gam(edge_foroh_270mT+year),eps(.),e(.),d(.),p(full_id+rain)	1086.65	7.31	< 0.01	0.03	33
psi(.),gam(edge_foroh_270m+year),eps(.),e(.),d(.),p(full_id+rain)	1086.71	7.37	< 0.01	0.03	33
psi(.),gam(prop_oh_540m+year),eps(.),e(.),d(.),p(full_id+rain)	1086.74	7.40	< 0.01	0.02	33
psi(.),gam(edge_foroh_3kmT+year),eps(.),e(.),d(.),p(full_id+rain)	1086.75	7.41	< 0.01	0.02	33
psi(.),gam(road_other_5km+year),eps(.),e(.),d(.),p(full_id+rain)	1086.79	7.45	< 0.01	0.02	33
psi(.),gam(prop_mesic_3kmT+year),eps(.),e(.),d(.),p(full_id+rain)	1086.83	7.49	< 0.01	0.02	33
psi(.),gam(prop_ag_5kmT+year),eps(.),e(.),d(.),p(full_id+rain)	1086.83	7.49	< 0.01	0.02	33
psi(.),gam(roads_local_5km+year),eps(.),e(.),d(.),p(full_id+rain)	1086.87	7.53	< 0.01	0.02	33
psi(.),gam(road_local_1km+year),eps(.),e(.),d(.),p(full_id+rain)	1086.87	7.53	< 0.01	0.02	33
psi(.),gam(edge_foroh_3km+year),eps(.),e(.),d(.),p(full_id+rain)	1086.88	7.54	< 0.01	0.02	33
psi(.),gam(prop_oh_540mT+year),eps(.),e(.),d(.),p(full_id+rain)	1086.88	7.54	< 0.01	0.02	33
psi(.),gam(edge_forag_5kmT+year),eps(.),e(.),d(.),p(full_id+rain)	1086.89	7.55	< 0.01	0.02	33
psi(.),gam(prop_rip_5km+year),eps(.),e(.),d(.),p(full_id+rain)	1086.90	7.56	< 0.01	0.02	33

psi(.),gam(edge_foroh_540m+year),eps(.),e(.),d(.),p(full_id+rain)	1086.91	7.57	< 0.01	0.02	33
psi(.),gam(edge_foroh_5km+year),eps(.),e(.),d(.),p(full_id+rain)	1086.91	7.57	< 0.01	0.02	33
psi(.),gam(road_local_5kmT+year),eps(.),e(.),d(.),p(full_id+rain)	1086.92	7.58	< 0.01	0.02	33
psi(.),gam(prop_mesic_5km+year),eps(.),e(.),d(.),p(full_id+rain)	1086.94	7.60	< 0.01	0.02	33
psi(.),gam(prop_oh_5km+year),eps(.),e(.),d(.),p(full_id+rain)	1086.94	7.60	< 0.01	0.02	33
psi(.),gam(edge_foroh_5kmT+year),eps(.),e(.),d(.),p(full_id+rain)	1086.95	7.61	< 0.01	0.02	33
psi(.),gam(prop_oh_5kmT+year),eps(.),e(.),d(.),p(full_id+rain)	1086.95	7.61	< 0.01	0.02	33
psi(.),gam(edge_forag_5km+year),eps(.),e(.),d(.),p(full_id+rain)	1086.98	7.64	< 0.01	0.02	33
psi(.),gam(road_other_1kmT+year),eps(.),e(.),d(.),p(full_id+rain)	1086.98	7.64	< 0.01	0.02	33
psi(.),gam(nectar+year),eps(.),e(.),d(.),p(full_id+rain)	1086.99	7.65	< 0.01	0.02	33
psi(.),gam(prop_oh_3kmT+year),eps(.),e(.),d(.),p(full_id+rain)	1087.00	7.66	< 0.01	0.02	33
psi(.),gam(edge_foroh_540mT+year),eps(.),e(.),d(.),p(full_id+rain)	1087.00	7.66	< 0.01	0.02	33
psi(.),gam(prop_oh_1km+year),eps(.),e(.),d(.),p(full_id+rain)	1087.00	7.66	< 0.01	0.02	33
psi(.),gam(road_local_3kmT+year),eps(.),e(.),d(.),p(full_id+rain)	1087.01	7.67	< 0.01	0.02	33
psi(.),gam(road_local_1kmT+year),eps(.),e(.),d(.),p(full_id+rain)	1087.01	7.67	< 0.01	0.02	33
psi(.),gam(prop_oh_3km+year),eps(.),e(.),d(.),p(full_id+rain)	1087.01	7.67	< 0.01	0.02	33
psi(.),gam(roads_local_3km+year),eps(.),e(.),d(.),p(full_id+rain)	1087.02	7.68	< 0.01	0.02	33
psi(.),gam(prop_oh_1kmT+year),eps(.),e(.),d(.),p(full_id+rain)	1087.02	7.68	< 0.01	0.02	33
psi(.),gam(prop_rip_5kmT+year),eps(.),e(.),d(.),p(full_id+rain)	1087.02	7.68	< 0.01	0.02	33
psi(.),gam(edge_foroh_1km+year),eps(.),e(.),d(.),p(full_id+rain)	1087.02	7.68	< 0.01	0.02	33
psi(.),gam(prop_succ_3km+year),eps(.),e(.),d(.),p(full_id+rain)	1087.03	7.69	< 0.01	0.02	33
psi(.),gam(road_other_1km+year),eps(.),e(.),d(.),p(full_id+rain)	1087.03	7.69	< 0.01	0.02	33
psi(.),gam(edge_foroh_1kmT+year),eps(.),e(.),d(.),p(full_id+rain)	1087.03	7.69	< 0.01	0.02	33
psi(.),gam(prop_mesic_3km+year),eps(.),e(.),d(.),p(full_id+rain)	1087.03	7.69	< 0.01	0.02	33
psi(.),gam(prop_succ_540mQ+year),eps(.),e(.),d(.),p(full_id+rain)	1087.04	7.70	< 0.01	0.02	34
psi(.),gam(prop_oh_270mQ+year),eps(.),e(.),d(.),p(full_id+rain)	1087.11	7.77	< 0.01	0.02	34

psi(.),gam(prop_succ_1kmQ+year),eps(.),e(.),d(.),p(full_id+rain)	1087.40	8.06	< 0.01	0.02	34
psi(.),gam(edge_foroh_5kmQ+year),eps(.),e(.),d(.),p(full_id+rain)	1087.43	8.09	< 0.01	0.02	34
psi(.),gam(prop_oh_540mQ+year),eps(.),e(.),d(.),p(full_id+rain)	1087.45	8.11	< 0.01	0.02	34
psi(.),gam(prop_oh_3kmQ+year),eps(.),e(.),d(.),p(full_id+rain)	1087.62	8.28	< 0.01	0.02	34
psi(.),gam(prop_rip_1kmQ+year),eps(.),e(.),d(.),p(full_id+rain)	1087.63	8.29	< 0.01	0.02	34
psi(.),gam(edge_foroh_540mQ+year),eps(.),e(.),d(.),p(full_id+rain)	1087.69	8.35	< 0.01	0.02	34
psi(.),gam(prop_mesic_1kmQ+year),eps(.),e(.),d(.),p(full_id+rain)	1087.93	8.59	< 0.01	0.01	34
psi(.),gam(prop_rip_3kmQ+year),eps(.),e(.),d(.),p(full_id+rain)	1088.04	8.70	< 0.01	0.01	34
psi(.),gam(edge_forag_3kmQ+year),eps(.),e(.),d(.),p(full_id+rain)	1088.06	8.72	< 0.01	0.01	34
psi(.),gam(prop_mesic_5kmQ+year),eps(.),e(.),d(.),p(full_id+rain)	1088.32	8.98	< 0.01	0.01	34
psi(.),gam(edge_foroh_270mQ+year),eps(.),e(.),d(.),p(full_id+rain)	1088.33	8.99	< 0.01	0.01	34
psi(.),gam(road_local_270mQ+year),eps(.),e(.),d(.),p(full_id+rain)	1088.34	9.00	< 0.01	0.01	34
psi(.),gam(prop_succ_270mQ+year),eps(.),e(.),d(.),p(full_id+rain)	1088.41	9.07	< 0.01	0.01	34
psi(.),gam(road_local_1kmQ+year),eps(.),e(.),d(.),p(full_id+rain)	1088.59	9.25	< 0.01	0.01	34
psi(.),gam(prop_oh_5kmQ+year),eps(.),e(.),d(.),p(full_id+rain)	1088.71	9.37	< 0.01	0.01	34
psi(.),gam(road_other_5kmQ+year),eps(.),e(.),d(.),p(full_id+rain)	1088.73	9.39	< 0.01	0.01	34
psi(.),gam(road_local_5kmQ+year),eps(.),e(.),d(.),p(full_id+rain)	1088.8	9.46	< 0.01	0.01	34
psi(.),gam(edge_forag_5kmQ+year),eps(.),e(.),d(.),p(full_id+rain)	1088.94	9.60	< 0.01	0.01	34
psi(.),gam(road_local_540mQ+year),eps(.),e(.),d(.),p(full_id+rain)	1089.45	10.11	< 0.01	< 0.01	34
psi(.),gam(prop_oh_1kmQ+year),eps(.),e(.),d(.),p(full_id+rain)	1091.94	12.60	< 0.01	< 0.01	34
psi(.),gam(edge_foroh_1kmQ+year),eps(.),e(.),d(.),p(full_id+rain)	1092.66	13.32	< 0.01	< 0.01	34

Appendix 8: Strengths of support for univariate models of colonization of *P. glaucus* while keeping the best detection model constant.

Psi = occupancy, p = detection, gam = colonization, eps = extinction, e = entry, and d = departure, survey[int_p6] = survey 6 set as intercept, Q = quadratic function ($x + x^2$), T = a pseudo-threshold function ($\ln[x]$), edge_foroh = edge density forest-open herbaceous, prop_upland = proportional upland, prop_flood = proportion floodplain, prop_ag = proportion agriculture, prop_succ = proportion successional, edge_forag = edge density forest-agriculture, lidar = structural heterogeneity 0.3-3.0m, prop_rip = proportion riparian, prop_mesic = proportion mesic, road_other = other roads, road_local = local roads, prop_oh = proportion open herbaceous, and AIC = Akaike's Information Criterion adjusted for sample size, ΔAIC = difference from the top model AIC, and $AIC\omega$ = model weight.

Model	AIC	ΔAIC	$AIC\omega$	Model Likelihood	Number of parameters
psi(.),gam(prop_oh_3km(gam2=int)),eps(.),e(.),d(.),p(season+survey[int_p6])	1177.58	0.00	0.17	1.00	16
psi(.),gam(road_local_3km(gam2=int)),eps(.),e(.),d(.),p(season+survey[int_p6])	1178.58	1.00	0.10	0.61	16
psi(.),gam(prop_oh_3kmQ(gam2=int)),eps(.),e(.),d(.),p(season+survey[int_p6])	1179.19	1.61	0.08	0.45	17
psi(.),gam(prop_oh_1km(gam2=int)),eps(.),e(.),d(.),p(season+survey[int_p6])	1179.73	2.15	0.06	0.34	16
psi(.),gam(prop_oh_1kmQ(gam2=int)),eps(.),e(.),d(.),p(season+survey[int_p6])	1179.73	2.15	0.06	0.34	17
psi(.),gam(prop_oh_5km(gam2=int)),eps(.),e(.),d(.),p(season+survey[int_p6])	1179.77	2.19	0.06	0.33	16
psi(.),gam(road_local_3kmQ(gam2=int)),eps(.),e(.),d(.),p(season+survey[int_p6])	1180.38	2.80	0.04	0.25	17
psi(.),gam(prop_succ_3km(gam2=int)),eps(.),e(.),d(.),p(season+survey[int_p6])	1181.12	3.54	0.03	0.17	16
psi(.),gam(road_local_5kmQ(gam2=int)),eps(.),e(.),d(.),p(season+survey[int_p6])	1181.15	3.57	0.03	0.17	17
psi(.),gam(edge_foroh_1kmQ(gam2=int)),eps(.),e(.),d(.),p(season+survey[int_p6])	1181.33	3.75	0.03	0.15	17

psi(.),gam(edge_foroh_5kmQ(gam2=int)),eps(.),e(.),d(.),p(season+survey[int_p6])	1181.50	3.92	0.02	0.14	17
psi(.),gam(road_local_5km(gam2=int)),eps(.),e(.),d(.),p(season+survey[int_p6])	1181.70	4.12	0.02	0.13	16
psi(.),gam(prop_oh_5kmQ(gam2=int)),eps(.),e(.),d(.),p(season+survey[int_p6])	1181.73	4.15	0.02	0.13	17
psi(.),gam(road_local_5kmT(gam2=int)),eps(.),e(.),d(.),p(season+survey[int_p6])	1181.95	4.37	0.02	0.11	16
psi(.),gam(edge_foroh_3km(gam2=int)),eps(.),e(.),d(.),p(season+survey[int_p6])	1181.98	4.40	0.02	0.11	16
psi(.),gam(edge_foroh_3kmT(gam2=int)),eps(.),e(.),d(.),p(season+survey[int_p6])	1182.02	4.44	0.02	0.11	16
psi(.),gam(road_other_1km(gam2=int)),eps(.),e(.),d(.),p(season+survey[int_p6])	1182.34	4.76	0.02	0.09	16
psi(.),gam(road_other_3km(gam2=int)),eps(.),e(.),d(.),p(season+survey[int_p6])	1182.34	4.76	0.02	0.09	16
psi(.),gam(road_other_1kmT(gam2=int)),eps(.),e(.),d(.),p(season+survey[int_p6] + nectar)	1182.36	4.78	0.02	0.09	16
psi(.),gam(edge_forag_5kmQ(gam2=int)),eps(.),e(.),d(.),p(season+survey[int_p6])	1182.85	5.27	0.01	0.07	17
psi(.),gam(prop_ag_3kmQ(gam2=int)),eps(.),e(.),d(.),p(season+survey[int_p6] + nectar)	1183.15	5.57	0.01	0.06	17
psi(.),gam(prop_rip_3km(gam2=int)),eps(.),e(.),d(.),p(season+survey[int_p6] + nectar)	1183.57	5.99	0.01	0.05	16
psi(.),gam(prop_rip_3kmT(gam2=int)),eps(.),e(.),d(.),p(season+survey[int_p6] + nectar)	1183.72	6.14	0.01	0.05	16
psi(.),gam(edge_foroh_3kmQ(gam2=int)),eps(.),e(.),d(.),p(season+survey[int_p6] + nectar)	1183.97	6.39	0.01	0.04	17
psi(.),gam(edge_foroh_1kmT(gam2=int)),eps(.),e(.),d(.),p(season+survey[int_p6] + nectar)	1184.01	6.43	0.01	0.04	16
psi(.),gam(road_local_540m(gam2=int)),eps(.),e(.),d(.),p(season+survey[int_p6])	1184.05	6.47	0.01	0.04	16
psi(.),gam(road_local_540mT(gam2=int)),eps(.),e(.),d(.),p(season+survey[int_p6])	1184.10	6.52	0.01	0.04	16
psi(.),gam(road_other_1kmQ(gam2=int)),eps(.),e(.),d(.),p(season+survey[int_p6] + nectar)	1184.31	6.73	0.01	0.03	17
psi(.),gam(lidar(gam2=int)),eps(.),e(.),d(.),p(season+survey[int_p6] + nectar)	1184.88	7.30	< 0.01	0.03	16
psi(.),gam(lidar(gam2=int)),eps(.),e(.),d(.),p(season+survey[int_p6])	1184.88	7.30	< 0.01	0.03	16
psi(.),gam(edge_foroh_1km(gam2=int)),eps(.),e(.),d(.),p(season+survey[int_p6] + nectar)	1185.21	7.63	< 0.01	0.02	16
psi(.),gam(lidarT(gam2=int)),eps(.),e(.),d(.),p(season+survey[int_p6] + nectar)	1185.27	7.69	< 0.01	0.02	16
psi(.),gam(prop_rip_3kmQ(gam2=int)),eps(.),e(.),d(.),p(season+survey[int_p6] + nectar)	1185.44	7.86	< 0.01	0.02	17
psi(.),gam(prop_flood_5km(gam2=int)),eps(.),e(.),d(.),p(season+survey[int_p6] + nectar)	1185.84	8.26	< 0.01	0.02	16
psi(.),gam(prop_rip_1km(gam2=int)),eps(.),e(.),d(.),p(season+survey[int_p6] + nectar)	1185.85	8.27	< 0.01	0.02	16
psi(.),gam(prop_flood_5kmT(gam2=int)),eps(.),e(.),d(.),p(season+survey[int_p6] + nectar)	1185.85	8.27	< 0.01	0.02	16

psi(.),gam(prop_mesic_3km(gam2=int)),eps(.),e(.),d(.),p(season+survey[int_p6] + nectar)	1185.88	8.30	< 0.01	0.02	16
psi(.),gam(prop_rip_1kmQ(gam2=int)),eps(.),e(.),d(.),p(season+survey[int_p6] + nectar)	1185.90	8.32	< 0.01	0.02	17
psi(.),gam(prop_mesic_5kmT(gam2=int)),eps(.),e(.),d(.),p(season+survey[int_p6] + nectar)	1185.96	8.38	< 0.01	0.02	16
psi(.),gam(road_local_540mQ(gam2=int)),eps(.),e(.),d(.),p(season+survey[int_p6] + nectar)	1186.03	8.45	< 0.01	0.01	17
psi(.),gam(road_local_270m(gam2=int)),eps(.),e(.),d(.),p(season+survey[int_p6] + nectar)	1186.07	8.49	< 0.01	0.01	16
psi(.),gam(prop_succ_1km(gam2=int)),eps(.),e(.),d(.),p(season+survey[int_p6] + nectar)	1186.08	8.50	< 0.01	0.01	16
psi(.),gam(prop_rip_1kmT(gam2=int)),eps(.),e(.),d(.),p(season+survey[int_p6] + nectar)	1186.17	8.59	< 0.01	0.01	16
psi(.),gam(prop_succ_1kmT(gam2=int)),eps(.),e(.),d(.),p(season+survey[int_p6] + nectar)	1186.44	8.86	< 0.01	0.01	16
psi(.),gam(edge_foroh_270mT(gam2=int)),eps(.),e(.),d(.),p(season+survey[int_p6] + nectar)	1186.55	8.97	< 0.01	0.01	16
psi(.),gam(prop_flood_3kmT(gam2=int)),eps(.),e(.),d(.),p(season+survey[int_p6] + nectar)	1186.59	9.01	< 0.01	0.01	16
psi(.),gam(road_local_270mQ(gam2=int)),eps(.),e(.),d(.),p(season+survey[int_p6] + nectar)	1186.62	9.04	< 0.01	0.01	17
psi(.),gam(prop_flood_3km(gam2=int)),eps(.),e(.),d(.),p(season+survey[int_p6] + nectar)	1186.64	9.06	< 0.01	0.01	16
psi(.),gam(prop_mesic_3kmT(gam2=int)),eps(.),e(.),d(.),p(season+survey[int_p6] + nectar)	1186.65	9.07	< 0.01	0.01	16
psi(.),gam(prop_oh_270mT(gam2=int)),eps(.),e(.),d(.),p(season+survey[int_p6] + nectar)	1186.69	9.11	< 0.01	0.01	16
psi(.),gam(road_local_270mT(gam2=int)),eps(.),e(.),d(.),p(season+survey[int_p6] + nectar)	1186.71	9.13	< 0.01	0.01	16
psi(.),gam(prop_oh_540mT(gam2=int)),eps(.),e(.),d(.),p(season+survey[int_p6] + nectar)	1186.78	9.20	< 0.01	0.01	16
psi(.),gam(edge_forag_3km(gam2=int)),eps(.),e(.),d(.),p(season+survey[int_p6] + nectar)	1187.01	9.43	< 0.01	0.01	16
psi(.),gam(prop_flood_270mQ(gam2=int)),eps(.),e(.),d(.),p(season+survey[int_p6] + nectar)	1187.02	9.44	< 0.01	0.01	17
psi(.),gam(edge_foroh_270m(gam2=int)),eps(.),e(.),d(.),p(season+survey[int_p6] + nectar)	1187.03	9.45	< 0.01	0.01	16
psi(.),gam(prop_oh_540m(gam2=int)),eps(.),e(.),d(.),p(season+survey[int_p6] + nectar)	1187.11	9.53	< 0.01	0.01	16
psi(.),gam(prop_mesic_5kmQ(gam2=int)),eps(.),e(.),d(.),p(season+survey[int_p6] + nectar)	1187.12	9.54	< 0.01	0.01	17
psi(.),gam(edge_forag_3kmQ(gam2=int)),eps(.),e(.),d(.),p(season+survey[int_p6] + nectar)	1187.21	9.63	< 0.01	0.01	17
psi(.),gam(prop_flood_1kmQ(gam2=int)),eps(.),e(.),d(.),p(season+survey[int_p6] + nectar)	1187.21	9.63	< 0.01	0.01	17
psi(.),gam(edge_foroh_540mT(gam2=int)),eps(.),e(.),d(.),p(season+survey[int_p6] + nectar)	1187.28	9.70	< 0.01	0.01	16
psi(.),gam(prop_mesic_5km(gam2=int)),eps(.),e(.),d(.),p(season+survey[int_p6] + nectar)	1187.48	9.90	< 0.01	0.01	16
psi(.),gam(prop_ag_5km(gam2=int)),eps(.),e(.),d(.),p(season+survey[int_p6] + nectar)	1187.49	9.91	< 0.01	0.01	16

psi(.),gam(prop_flood_540m(gam2=int)),eps(.),e(.),d(.),p(season+survey[int_p6] + nectar)	1187.59	10.01	< 0.01	0.01	16
psi(.),gam(prop_rip_270mQ(gam2=int)),eps(.),e(.),d(.),p(season+survey[int_p6] + nectar)	1187.63	10.05	< 0.01	0.01	17
psi(.),gam(edge_forag_3kmT(gam2=int)),eps(.),e(.),d(.),p(season+survey[int_p6] + nectar)	1187.68	10.1	< 0.01	0.01	16
psi(.),gam(edge_foroh_540m(gam2=int)),eps(.),e(.),d(.),p(season+survey[int_p6] + nectar)	1187.75	10.17	< 0.01	0.01	16
psi(.),gam(prop_flood_540mT(gam2=int)),eps(.),e(.),d(.),p(season+survey[int_p6] + nectar)	1187.76	10.18	< 0.01	0.01	16
psi(.),gam(edge_foroh_270mQ(gam2=int)),eps(.),e(.),d(.),p(season+survey[int_p6] + nectar)	1187.77	10.19	< 0.01	0.01	17
psi(.),gam(prop_ag_540mQ(gam2=int)),eps(.),e(.),d(.),p(season+survey[int_p6] + nectar)	1187.79	10.21	< 0.01	0.01	17
psi(.),gam(prop_ag_5kmT(gam2=int)),eps(.),e(.),d(.),p(season+survey[int_p6] + nectar)	1187.79	10.21	< 0.01	0.01	16
psi(.),gam(edge_forag_5kmT(gam2=int)),eps(.),e(.),d(.),p(season+survey[int_p6] + nectar)	1187.8	10.22	< 0.01	0.01	16
psi(.),gam(prop_mesic_3kmQ(gam2=int)),eps(.),e(.),d(.),p(season+survey[int_p6] + nectar)	1187.84	10.26	< 0.01	0.01	17
psi(.),gam(prop_flood_5kmQ(gam2=int)),eps(.),e(.),d(.),p(season+survey[int_p6] + nectar)	1187.84	10.26	< 0.01	0.01	17
psi(.),gam(prop_flood_1km(gam2=int)),eps(.),e(.),d(.),p(season+survey[int_p6] + nectar)	1187.89	10.31	< 0.01	0.01	16
psi(.),gam(road_other_5kmQ(gam2=int)),eps(.),e(.),d(.),p(season+survey[int_p6] + nectar)	1187.94	10.36	< 0.01	0.01	17
psi(.),gam(prop_succ_1kmQ(gam2=int)),eps(.),e(.),d(.),p(season+survey[int_p6] + nectar)	1188.00	10.42	< 0.01	0.01	17
psi(.),gam(prop_flood_1kmT(gam2=int)),eps(.),e(.),d(.),p(season+survey[int_p6] + nectar)	1188.05	10.47	< 0.01	0.01	16
psi(.),gam(edge_forag_540m(gam2=int)),eps(.),e(.),d(.),p(season+survey[int_p6] + nectar)	1188.08	10.50	< 0.01	0.01	16
psi(.),gam(edge_forag_5km(gam2=int)),eps(.),e(.),d(.),p(season+survey[int_p6] + nectar)	1188.15	10.57	< 0.01	0.01	16
psi(.),gam(canopyT(gam2=int)),eps(.),e(.),d(.),p(season+survey[int_p6] + nectar)	1188.17	10.59	< 0.01	0.01	16
psi(.),gam(prop_flood_270m(gam2=int)),eps(.),e(.),d(.),p(season+survey[int_p6] + nectar)	1188.24	10.66	< 0.01	< 0.01	16
psi(.),gam(prop_ag_3km(gam2=int)),eps(.),e(.),d(.),p(season+survey[int_p6] + nectar)	1188.27	10.69	< 0.01	< 0.01	16
psi(.),gam(prop_oh_540mQ(gam2=int)),eps(.),e(.),d(.),p(season+survey[int_p6] + nectar)	1188.31	10.73	< 0.01	< 0.01	17
psi(.),gam(edge_forag_540mT(gam2=int)),eps(.),e(.),d(.),p(season+survey[int_p6] + nectar)	1188.34	10.76	< 0.01	< 0.01	16
psi(.),gam(prop_mesic_270m(gam2=int)),eps(.),e(.),d(.),p(season+survey[int_p6] + nectar)	1188.35	10.77	< 0.01	< 0.01	16
psi(.),gam(prop_flood_270mT(gam2=int)),eps(.),e(.),d(.),p(season+survey[int_p6] + nectar)	1188.44	10.86	< 0.01	< 0.01	16
psi(.),gam(rcanopy(gam2=int)),eps(.),e(.),d(.),p(season+survey[int_p6] + nectar)	1188.54	10.96	< 0.01	< 0.01	16
psi(.),gam(prop_flood_3kmQ(gam2=int)),eps(.),e(.),d(.),p(season+survey[int_p6] + nectar)	1188.59	11.01	< 0.01	< 0.01	17

psi(.),gam(prop_ag_5kmQ(gam2=int)),eps(.),e(.),d(.),p(season+survey[int_p6] + nectar)	1188.67	11.09	< 0.01	< 0.01	17
psi(.),gam(road_other_540m(gam2=int)),eps(.),e(.),d(.),p(season+survey[int_p6] + nectar)	1188.77	11.19	< 0.01	< 0.01	16
psi(.),gam(.),eps(.),e(.),d(.),p(season+survey[int_p6] + nectar)	1188.77	11.19	< 0.01	< 0.01	14
psi(.),gam(.),eps(.),e(.),d(.),p(season+survey[int_p6])	1188.77	11.19	< 0.01	< 0.01	14
psi(.),gam(road_other_540mT(gam2=int)),eps(.),e(.),d(.),p(season+survey[int_p6] + nectar)	1188.78	11.20	< 0.01	< 0.01	16
psi(.),gam(prop_rip_5kmT(gam2=int)),eps(.),e(.),d(.),p(season+survey[int_p6] + nectar)	1188.82	11.24	< 0.01	< 0.01	16
psi(.),gam(prop_ag_3kmT(gam2=int)),eps(.),e(.),d(.),p(season+survey[int_p6] + nectar)	1188.82	11.24	< 0.01	< 0.01	16
psi(.),gam(edge_foroh_540mQ(gam2=int)),eps(.),e(.),d(.),p(season+survey[int_p6] + nectar)	1188.83	11.25	< 0.01	< 0.01	17
psi(.),gam(prop_rip_540m(gam2=int)),eps(.),e(.),d(.),p(season+survey[int_p6] + nectar)	1188.83	11.25	< 0.01	< 0.01	16
psi(.),gam(edge_forag_1kmQ(gam2=int)),eps(.),e(.),d(.),p(season+survey[int_p6] + nectar)	1188.84	11.26	< 0.01	< 0.01	17
psi(.),gam(prop_mesic_270mT(gam2=int)),eps(.),e(.),d(.),p(season+survey[int_p6] + nectar)	1188.96	11.38	< 0.01	< 0.01	16
psi(.),gam(edge_forag_540mQ(gam2=int)),eps(.),e(.),d(.),p(season+survey[int_p6] + nectar)	1188.98	11.40	< 0.01	< 0.01	17
psi(.),gam(prop_rip_540mT(gam2=int)),eps(.),e(.),d(.),p(season+survey[int_p6] + nectar)	1189.00	11.42	< 0.01	< 0.01	16
psi(.),gam(prop_ag_540m(gam2=int)),eps(.),e(.),d(.),p(season+survey[int_p6] + nectar)	1189.02	11.44	< 0.01	< 0.01	16
psi(.),gam(prop_ag_270m(gam2=int)),eps(.),e(.),d(.),p(season+survey[int_p6] + nectar)	1189.07	11.49	< 0.01	< 0.01	16
psi(.),gam(edge_forag_1km(gam2=int)),eps(.),e(.),d(.),p(season+survey[int_p6] + nectar)	1189.12	11.54	< 0.01	< 0.01	16
psi(.),gam(prop_rip_270m(gam2=int)),eps(.),e(.),d(.),p(season+survey[int_p6] + nectar)	1189.14	11.56	< 0.01	< 0.01	16
psi(.),gam(prop_succ_540mT(gam2=int)),eps(.),e(.),d(.),p(season+survey[int_p6] + nectar)	1189.22	11.64	< 0.01	< 0.01	16
psi(.),gam(prop_succ_540m(gam2=int)),eps(.),e(.),d(.),p(season+survey[int_p6] + nectar)	1189.23	11.65	< 0.01	< 0.01	16
psi(.),gam(prop_ag_270mT(gam2=int)),eps(.),e(.),d(.),p(season+survey[int_p6] + nectar)	1189.26	11.68	< 0.01	< 0.01	16
psi(.),gam(prop_rip_5km(gam2=int)),eps(.),e(.),d(.),p(season+survey[int_p6] + nectar)	1189.28	11.70	< 0.01	< 0.01	16
psi(.),gam(prop_ag_540mT(gam2=int)),eps(.),e(.),d(.),p(season+survey[int_p6] + nectar)	1189.33	11.75	< 0.01	< 0.01	16
psi(.),gam(prop_rip_270mT(gam2=int)),eps(.),e(.),d(.),p(season+survey[int_p6] + nectar)	1189.34	11.76	< 0.01	< 0.01	16
psi(.),gam(edge_forag_270m(gam2=int)),eps(.),e(.),d(.),p(season+survey[int_p6] + nectar)	1189.38	11.80	< 0.01	< 0.01	16
psi(.),gam(prop_mesic_1km(gam2=int)),eps(.),e(.),d(.),p(season+survey[int_p6] + nectar)	1189.46	11.88	< 0.01	< 0.01	16
psi(.),gam(prop_mesic_1kmT(gam2=int)),eps(.),e(.),d(.),p(season+survey[int_p6] + nectar)	1189.46	11.88	< 0.01	< 0.01	16

psi(.),gam(edge_forag_1kmT(gam2=int)),eps(.),e(.),d(.),p(season+survey[int_p6] + nectar)	1189.47	11.89	< 0.01	< 0.01	16
psi(.),gam(edge_forag_270mT(gam2=int)),eps(.),e(.),d(.),p(season+survey[int_p6] + nectar)	1189.50	11.92	< 0.01	< 0.01	16
psi(.),gam(road_other_3kmT(gam2=int)),eps(.),e(.),d(.),p(season+survey[int_p6] + nectar)	1189.53	11.95	< 0.01	< 0.01	16
psi(.),gam(prop_ag_1km(gam2=int)),eps(.),e(.),d(.),p(season+survey[int_p6] + nectar)	1189.62	12.04	< 0.01	< 0.01	16
psi(.),gam(road_other_5km(gam2=int)),eps(.),e(.),d(.),p(season+survey[int_p6] + nectar)	1189.66	12.08	< 0.01	< 0.01	16
psi(.),gam(prop_ag_270mQ(gam2=int)),eps(.),e(.),d(.),p(season+survey[int_p6] + nectar)	1189.67	12.09	< 0.01	< 0.01	17
psi(.),gam(prop_ag_1kmT(gam2=int)),eps(.),e(.),d(.),p(season+survey[int_p6] + nectar)	1189.78	12.20	< 0.01	< 0.01	16
psi(.),gam(prop_succ_270mT(gam2=int)),eps(.),e(.),d(.),p(season+survey[int_p6] + nectar)	1189.80	12.22	< 0.01	< 0.01	16
psi(.),gam(prop_succ_270m(gam2=int)),eps(.),e(.),d(.),p(season+survey[int_p6] + nectar)	1189.85	12.27	< 0.01	< 0.01	16
psi(.),gam(road_other_5kmT(gam2=int)),eps(.),e(.),d(.),p(season+survey[int_p6] + nectar)	1189.86	12.28	< 0.01	< 0.01	16
psi(.),gam(prop_mesic_540mT(gam2=int)),eps(.),e(.),d(.),p(season+survey[int_p6] + nectar)	1189.86	12.28	< 0.01	< 0.01	16
psi(.),gam(prop_rip_540mQ(gam2=int)),eps(.),e(.),d(.),p(season+survey[int_p6] + nectar)	1190.14	12.56	< 0.01	< 0.01	17
psi(.),gam(prop_rip_5kmQ(gam2=int)),eps(.),e(.),d(.),p(season+survey[int_p6] + nectar)	1190.53	12.95	< 0.01	< 0.01	17
psi(.),gam(prop_ag_1kmQ(gam2=int)),eps(.),e(.),d(.),p(season+survey[int_p6] + nectar)	1190.63	13.05	< 0.01	< 0.01	17
psi(.),gam(road_other_540mQ(gam2=int)),eps(.),e(.),d(.),p(season+survey[int_p6] + nectar)	1190.77	13.19	< 0.01	< 0.01	17
psi(.),gam(prop_mesic_1kmQ(gam2=int)),eps(.),e(.),d(.),p(season+survey[int_p6] + nectar)	1190.86	13.28	< 0.01	< 0.01	17
psi(.),gam(edge_forag_270mQ(gam2=int)),eps(.),e(.),d(.),p(season+survey[int_p6] + nectar)	1191.05	13.47	< 0.01	< 0.01	17
psi(.),gam(prop_succ_540mQ(gam2=int)),eps(.),e(.),d(.),p(season+survey[int_p6] + nectar)	1191.44	13.86	< 0.01	< 0.01	17
psi(.),gam(prop_succ_270mQ(gam2=int)),eps(.),e(.),d(.),p(season+survey[int_p6] + nectar)	1191.44	13.86	< 0.01	< 0.01	17
psi(.),gam(road_other_3kmQ(gam2=int)),eps(.),e(.),d(.),p(season+survey[int_p6] + nectar)	1191.56	13.98	< 0.01	< 0.01	17

Appendix 9: Strengths of support for univariate models of extinction of *E. marcellus* while keeping the best detection model constant.

Psi = occupancy, p = detection, gam = colonization, eps = extinction, e = entry, and d = departure, full_id = season*survey interaction, rain = days since rain, Q = quadratic function ($x + x^2$), T = a pseudo-threshold function ($\ln[x]$), edge_forwet = edge density forest-wetlands, prop_upland = proportion upland forest, prop_flood = proportion floodplain, edge_mdwet = edge density mixed/decid-forest, prop_conif = proportion coniferous forest, lidar = structural heterogeneity 0.3-3.0m, prop_wet = proportion wetland, basal_conif_canopy = basal area of coniferous canopy, count_conif_canopy = count of coniferous trees in canopy, and AIC = Akaike's Information Criterion adjusted for sample size, ΔAIC = difference from the top model AIC, and $AIC\omega$ = model weight.

Model	AIC	ΔAIC	$AIC\omega$	Model Likelihood	Number of parameters
psi(.),gam(.),eps(edge_forwet_5km+year),e(.),d(.),p(full_id+rain)	1075.63	0.00	0.19	1.00	33
psi(.),gam(.),eps(lidar_mean+year),e(.),d(.),p(full_id+rain)	1077.54	1.91	0.07	0.38	33
psi(.),gam(.),eps(prop_conif_5kmQ+year),e(.),d(.),p(full_id+rain)	1077.75	2.12	0.07	0.35	34
psi(.),gam(.),eps(lidarQ+year),e(.),d(.),p(full_id+rain)	1078.12	2.49	0.05	0.29	34
psi(.),gam(.),eps(prop_wet_3kmQ+year),e(.),d(.),p(full_id+rain)	1078.16	2.53	0.05	0.28	34
psi(.),gam(.),eps(edge_mdwet_5kmT+year),e(.),d(.),p(full_id+rain)	1078.19	2.56	0.05	0.28	33
psi(.),gam(.),eps(prop_upland_3km+year),e(.),d(.),p(full_id+rain)	1078.56	2.93	0.04	0.23	33
psi(.),gam(.),eps(prop_upland_270m+year),e(.),d(.),p(full_id+rain)	1078.80	3.17	0.04	0.20	33
psi(.),gam(.),eps(prop_upland_3kmT+year),e(.),d(.),p(full_id+rain)	1078.85	3.22	0.04	0.20	33
psi(.),gam(.),eps(prop_upland_270mT+year),e(.),d(.),p(full_id+rain)	1078.90	3.27	0.04	0.20	33
psi(.),gam(.),eps(edge_mdwet_5km+year),e(.),d(.),p(full_id+rain)	1078.98	3.35	0.04	0.19	33
psi(.),gam(.),eps(prop_wet_5km+year),e(.),d(.),p(full_id+rain)	1079.14	3.51	0.03	0.17	33

psi(.),gam(.),eps(prop_flood_3kmQ+year),e(.),d(.),p(full_id+rain)	1079.49	3.86	0.03	0.15	34
psi(.),gam(.),eps(prop_conif_1kmQ+year),e(.),d(.),p(full_id+rain)	1079.63	4.00	0.03	0.14	34
psi(.),gam(.),eps(prop_upland_270mQ+year),e(.),d(.),p(full_id+rain)	1079.70	4.07	0.02	0.13	34
psi(.),gam(.),eps(prop_flood_270m+year),e(.),d(.),p(full_id+rain)	1079.87	4.24	0.02	0.12	33
psi(.),gam(.),eps(prop_flood_270mT+year),e(.),d(.),p(full_id+rain)	1079.87	4.24	0.02	0.12	33
psi(.),gam(.),eps(prop_conif_3kmQ+year),e(.),d(.),p(full_id+rain)	1080.49	4.86	0.02	0.09	34
psi(.),gam(.),eps(prop_wet_270mQ+year),e(.),d(.),p(full_id+rain)	1081.10	5.47	0.01	0.06	34
psi(.),gam(.),eps(prop_flood_270mQ+year),e(.),d(.),p(full_id+rain)	1081.87	6.24	0.01	0.04	34
psi(.),gam(.),eps(prop_wet_540mQ+year),e(.),d(.),p(full_id+rain)	1081.92	6.29	0.01	0.04	34
psi(.),gam(.),eps(prop_wet_3kmT+year),e(.),d(.),p(full_id+rain)	1082.04	6.41	0.01	0.04	33
psi(.),gam(.),eps(prop_conif_540mQ+year),e(.),d(.),p(full_id+rain)	1082.23	6.60	0.01	0.04	34
psi(.),gam(.),eps(prop_flood_3km+year),e(.),d(.),p(full_id+rain)	1082.49	6.86	0.01	0.03	33
psi(.),gam(.),eps(prop_wet_3km+year),e(.),d(.),p(full_id+rain)	1082.49	6.86	0.01	0.03	33
psi(.),gam(.),eps(prop_flood_540mQ+year),e(.),d(.),p(full_id+rain)	1082.56	6.93	0.01	0.03	34
psi(.),gam(.),eps(prop_flood_3kmT+year),e(.),d(.),p(full_id+rain)	1082.92	7.29	< 0.01	0.03	33
psi(.),gam(.),eps(prop_conif_5km+year),e(.),d(.),p(full_id+rain)	1083.35	7.72	< 0.01	0.02	33
psi(.),gam(.),eps(prop_flood_1km+year),e(.),d(.),p(full_id+rain)	1083.51	7.88	< 0.01	0.02	33
psi(.),gam(.),eps(prop_flood_1kmT+year),e(.),d(.),p(full_id+rain)	1083.75	8.12	< 0.01	0.02	33
psi(.),gam(.),eps(edge_forwet_270m+year),e(.),d(.),p(full_id+rain)	1083.96	8.33	< 0.01	0.02	33
psi(.),gam(.),eps(edge_mdwet_270m+year),e(.),d(.),p(full_id+rain)	1084.05	8.42	< 0.01	0.01	33
psi(.),gam(.),eps(prop_conif_270mQ+year),e(.),d(.),p(full_id+rain)	1084.10	8.47	< 0.01	0.01	34
psi(.),gam(.),eps(prop_flood_540m+year),e(.),d(.),p(full_id+rain)	1084.15	8.52	< 0.01	0.01	33
psi(.),gam(.),eps(prop_flood_1kmQ+year),e(.),d(.),p(full_id+rain)	1084.24	8.61	< 0.01	0.01	34
psi(.),gam(.),eps(edge_forwet_270mT+year),e(.),d(.),p(full_id+rain)	1084.42	8.79	< 0.01	0.01	33
psi(.),gam(.),eps(edge_mdwet_270mT+year),e(.),d(.),p(full_id+rain)	1084.48	8.85	< 0.01	0.01	33
psi(.),gam(.),eps(prop_flood_540mT+year),e(.),d(.),p(full_id+rain)	1084.49	8.86	< 0.01	0.01	33

psi(.),gam(.),eps(.),e(.),d(.),p(full_id+rain)	1084.62	8.99	< 0.01	0.01	32
psi(.),gam(.),eps(prop_conif_3km+year),e(.),d(.),p(full_id+rain)	1084.63	9.00	< 0.01	0.01	33
psi(.),gam(.),eps(edge_forwet_3kmT+year),e(.),d(.),p(full_id+rain)	1084.70	9.07	< 0.01	0.01	33
psi(.),gam(.),eps(edge_forwet_3km+year),e(.),d(.),p(full_id+rain)	1084.84	9.21	< 0.01	0.01	33
psi(.),gam(.),eps(prop_conif_5kmT+year),e(.),d(.),p(full_id+rain)	1085.06	9.43	< 0.01	0.01	33
psi(.),gam(.),eps(edge_forwet_270mQ+year),e(.),d(.),p(full_id+rain)	1085.13	9.5	< 0.01	0.01	34
psi(.),gam(.),eps(edge_mdwet_3kmT+year),e(.),d(.),p(full_id+rain)	1085.17	9.54	< 0.01	0.01	33
psi(.),gam(.),eps(prop_conif_540m+year),e(.),d(.),p(full_id+rain)	1085.18	9.55	< 0.01	0.01	33
psi(.),gam(.),eps(prop_conif_270m+year),e(.),d(.),p(full_id+rain)	1085.22	9.59	< 0.01	0.01	33
psi(.),gam(.),eps(edge_mdwet_270mQ+year),e(.),d(.),p(full_id+rain)	1085.24	9.61	< 0.01	0.01	34
psi(.),gam(.),eps(edge_mdwet_3km+year),e(.),d(.),p(full_id+rain)	1085.48	9.85	< 0.01	0.01	33
psi(.),gam(.),eps(edge_mdwet_540mT+year),e(.),d(.),p(full_id+rain)	1085.51	9.88	< 0.01	0.01	33
psi(.),gam(.),eps(edge_forwet_540mT+year),e(.),d(.),p(full_id+rain)	1085.55	9.92	< 0.01	0.01	33
psi(.),gam(.),eps(edge_mdwet_540m+year),e(.),d(.),p(full_id+rain)	1085.55	9.92	< 0.01	0.01	33
psi(.),gam(.),eps(edge_forwet_540m+year),e(.),d(.),p(full_id+rain)	1085.67	10.04	< 0.01	0.01	33
psi(.),gam(.),eps(prop_conif_3kmT+year),e(.),d(.),p(full_id+rain)	1085.82	10.19	< 0.01	0.01	33
psi(.),gam(.),eps(prop_conif_270mT+year),e(.),d(.),p(full_id+rain)	1085.83	10.20	< 0.01	0.01	33
psi(.),gam(.),eps(prop_conif_1km+year),e(.),d(.),p(full_id+rain)	1085.84	10.21	< 0.01	0.01	33
psi(.),gam(.),eps(basal_conif_can+year),e(.),d(.),p(full_id+rain)	1085.86	10.23	< 0.01	0.01	33
psi(.),gam(.),eps(edge_forwet_1kmQ+year),e(.),d(.),p(full_id+rain)	1085.87	10.24	< 0.01	0.01	34
psi(.),gam(.),eps(edge_forwet_5kmQ+year),e(.),d(.),p(full_id+rain)	1085.87	10.24	< 0.01	0.01	34
psi(.),gam(.),eps(edge_forwet_3kmQ+year),e(.),d(.),p(full_id+rain)	1085.87	10.24	< 0.01	0.01	34
psi(.),gam(.),eps(prop_conif_540mT+year),e(.),d(.),p(full_id+rain)	1085.95	10.32	< 0.01	0.01	33
psi(.),gam(.),eps(prop_wet_540m+year),e(.),d(.),p(full_id+rain)	1086.13	10.50	< 0.01	0.01	33
psi(.),gam(.),eps(prop_flood_5km+year),e(.),d(.),p(full_id+rain)	1086.25	10.62	< 0.01	< 0.01	33
psi(.),gam(.),eps(basal_conif_cantpT+year),e(.),d(.),p(full_id+rain)	1086.26	10.63	< 0.01	< 0.01	33

psi(.),gam(.),eps(edge_mdwet_1kmQ+year),e(.),d(.),p(full_id+rain)	1086.28	10.65	< 0.01	< 0.01	34
psi(.),gam(.),eps(edge_mdwet_3kmQ+year),e(.),d(.),p(full_id+rain)	1086.29	10.66	< 0.01	< 0.01	34
psi(.),gam(.),eps(prop_wet_1km+year),e(.),d(.),p(full_id+rain)	1086.29	10.66	< 0.01	< 0.01	33
psi(.),gam(.),eps(prop_flood_5kmQ+year),e(.),d(.),p(full_id+rain)	1086.38	10.75	< 0.01	< 0.01	34
psi(.),gam(.),eps(prop_wet_1kmT+year),e(.),d(.),p(full_id+rain)	1086.39	10.76	< 0.01	< 0.01	33
psi(.),gam(.),eps(canopyT+year),e(.),d(.),p(full_id+rain)	1086.43	10.80	< 0.01	< 0.01	33
psi(.),gam(.),eps(count_conif_can+year),e(.),d(.),p(full_id+rain)	1086.46	10.83	< 0.01	< 0.01	33
psi(.),gam(.),eps(prop_wet_540mT+year),e(.),d(.),p(full_id+rain)	1086.46	10.83	< 0.01	< 0.01	33
psi(.),gam(.),eps(prop_flood_5kmT+year),e(.),d(.),p(full_id+rain)	1086.47	10.84	< 0.01	< 0.01	33
psi(.),gam(.),eps(edge_mdwet_1kmT+year),e(.),d(.),p(full_id+rain)	1086.50	10.87	< 0.01	< 0.01	33
psi(.),gam(.),eps(prop_conif_1kmT+year),e(.),d(.),p(full_id+rain)	1086.50	10.87	< 0.01	< 0.01	33
psi(.),gam(.),eps(edge_forwet_1kmT+year),e(.),d(.),p(full_id+rain)	1086.51	10.88	< 0.01	< 0.01	33
psi(.),gam(.),eps(count_conif_canT+year),e(.),d(.),p(full_id+rain)	1086.51	10.88	< 0.01	< 0.01	33
psi(.),gam(.),eps(prop_wet_270m+year),e(.),d(.),p(full_id+rain)	1086.58	10.95	< 0.01	< 0.01	33
psi(.),gam(.),eps(edge_mdwet_1km+year),e(.),d(.),p(full_id+rain)	1086.60	10.97	< 0.01	< 0.01	33
psi(.),gam(.),eps(edge_forwet_1km+year),e(.),d(.),p(full_id+rain)	1086.61	10.98	< 0.01	< 0.01	33
psi(.),gam(.),eps(canopy_cover+year),e(.),d(.),p(full_id+rain)	1086.61	10.98	< 0.01	< 0.01	33
psi(.),gam(.),eps(prop_wet_270mT+year),e(.),d(.),p(full_id+rain)	1086.61	10.98	< 0.01	< 0.01	33
psi(.),gam(.),eps(basal_conif_campQ+year),e(.),d(.),p(full_id+rain)	1086.73	11.10	< 0.01	< 0.01	34
psi(.),gam(.),eps(edge_forwet_540mQ+year),e(.),d(.),p(full_id+rain)	1087.43	11.80	< 0.01	< 0.01	34
psi(.),gam(.),eps(edge_mdwet_540mQ+year),e(.),d(.),p(full_id+rain)	1087.53	11.90	< 0.01	< 0.01	34
psi(.),gam(.),eps(canopyQ+year),e(.),d(.),p(full_id+rain)	1087.66	12.03	< 0.01	< 0.01	34
psi(.),gam(.),eps(count_conif_canQ+year),e(.),d(.),p(full_id+rain)	1088.33	12.70	< 0.01	< 0.01	34
psi(.),gam(.),eps(prop_wet_1kmQ+year),e(.),d(.),p(full_id+rain)	1089.95	14.32	< 0.01	< 0.01	34

Appendix 10: Strengths of support for univariate models of extinction of *P. glaucus* while keeping the best detection model constant.

Psi = occupancy, p = detection, gam = colonization, eps = extinction, e = entry, and d = departure, survey[int_p6] = survey 6 set as intercept, Q = quadratic function ($x + x^2$), T = a pseudo-threshold function ($\ln[x]$), edge_forwet = edge density forest-wetlands, edge_mdwet = edge density mixed/decid-forest, prop_conif = proportion coniferous forest, prop_wet = proportion wetland, basal_conif_canopy = basal area of coniferous canopy, count_conif_canopy = count of coniferous trees in canopy , and AIC = Akaike's Information Criterion adjusted for sample size, ΔAIC = difference from the top model AIC, and $AIC\omega$ = model weight.

Model	AIC	ΔAIC	$AIC\omega$	Model Likelihood	Number of parameters
psi(.),gam(.),eps(edge_forwet_540m(eps1=int)),e(.),d(.),p(season+survey[int_p6])	1184.53	0.00	0.09	1.00	17
psi(.),gam(.),eps(prop_wet_3km(eps1=int)),e(.),d(.),p(season+survey[int_p6])	1184.66	0.13	0.08	0.94	16
psi(.),gam(.),eps(prop_wet_3kmQ(eps1=int)),e(.),d(.),p(season+survey[int_p6])	1184.71	0.18	0.08	0.91	17
psi(.),gam(.),eps(prop_wet_3kmT(eps1=int)),e(.),d(.),p(season+survey[int_p6])	1184.72	0.19	0.08	0.91	16
psi(.),gam(.),eps(prop_conif_1km(eps1=int)),e(.),d(.),p(season+survey[int_p6])	1186.18	1.65	0.04	0.44	16
psi(.),gam(.),eps(prop_conif_1kmT(eps1=int)),e(.),d(.),p(season+survey[int_p6])	1186.28	1.75	0.04	0.42	16
psi(.),gam(.),eps(edge_mdwet_3km(eps1=int)),e(.),d(.),p(season+survey[int_p6])	1186.56	2.03	0.03	0.36	16
psi(.),gam(.),eps(edge_mdwet_3kmT(eps1=int)),e(.),d(.),p(season+survey[int_p6])	1186.91	2.38	0.03	0.30	16
psi(.),gam(.),eps(prop_wet_5kmQ(eps1=int)),e(.),d(.),p(season+survey[int_p6])	1187.04	2.51	0.03	0.29	17
psi(.),gam(.),eps(prop_wet_5km(eps1=int)),e(.),d(.),p(season+survey[int_p6])	1187.31	2.78	0.02	0.25	16
psi(.),gam(.),eps(prop_conif_3km(eps1=int)),e(.),d(.),p(season+survey[int_p6])	1187.41	2.88	0.02	0.24	16
psi(.),gam(.),eps(edge_mdwet_540m(eps1=int)),e(.),d(.),p(season+survey[int_p6])	1187.45	2.92	0.02	0.23	16
psi(.),gam(.),eps(prop_conif_3kmT(eps1=int)),e(.),d(.),p(season+survey[int_p6])	1187.47	2.94	0.02	0.23	16
psi(.),gam(.),eps(prop_wet_5kmT(eps1=int)),e(.),d(.),p(season+survey[int_p6])	1187.52	2.99	0.02	0.22	16

psi(.),gam(.),eps(edge_mdwet_540mT(eps1=int)),e(.),d(.),p(season+survey[int_p6])	1187.56	3.03	0.02	0.22	16
psi(.),gam(.),eps(prop_conif_1kmQ(eps1=int)),e(.),d(.),p(season+survey[int_p6])	1187.86	3.33	0.02	0.19	17
psi(.),gam(.),eps(edge_mdwet_1kmT(eps1=int)),e(.),d(.),p(season+survey[int_p6])	1188.14	3.61	0.01	0.16	16
psi(.),gam(.),eps(edge_mdwet_3kmQ(eps1=int)),e(.),d(.),p(season+survey[int_p6])	1188.14	3.61	0.01	0.16	17
psi(.),gam(.),eps(prop_conif_270mQ(eps1=int)),e(.),d(.),p(season+survey[int_p6])	1188.34	3.81	0.01	0.15	17
psi(.),gam(.),eps(edge_mdwet_1km(eps1=int)),e(.),d(.),p(season+survey[int_p6])	1188.37	3.84	0.01	0.15	16
psi(.),gam(.),eps(prop_wet_1kmT(eps1=int)),e(.),d(.),p(season+survey[int_p6])	1188.61	4.08	0.01	0.13	16
psi(.),gam(.),eps(.),e(.),d(.),p(season+survey[int_p6])	1188.77	4.24	0.01	0.12	14
psi(.),gam(.),eps(prop_wet_1km(eps1=int)),e(.),d(.),p(season+survey[int_p6])	1188.81	4.28	0.01	0.12	16
psi(.),gam(.),eps(prop_upland_5kmT(eps1=int)),e(.),d(.),p(season+survey[int_p6])	1188.82	4.29	0.01	0.12	16
psi(.),gam(.),eps(prop_upland_5km(eps1=int)),e(.),d(.),p(season+survey[int_p6])	1188.97	4.44	0.01	0.11	16
psi(.),gam(.),eps(edge_mdwet_5km(eps1=int)),e(.),d(.),p(season+survey[int_p6])	1189.03	4.5	0.01	0.11	16
psi(.),gam(.),eps(prop_conif_5kmT(eps1=int)),e(.),d(.),p(season+survey[int_p6])	1189.07	4.54	0.01	0.10	16
psi(.),gam(.),eps(prop_wet_540mT(eps1=int)),e(.),d(.),p(season+survey[int_p6])	1189.08	4.55	0.01	0.10	16
psi(.),gam(.),eps(prop_conif_3kmQ(eps1=int)),e(.),d(.),p(season+survey[int_p6])	1189.12	4.59	0.01	0.10	17
psi(.),gam(.),eps(edge_mdwet_540mQ(eps1=int)),e(.),d(.),p(season+survey[int_p6])	1189.20	4.67	0.01	0.10	17
psi(.),gam(.),eps(prop_conif_5km(eps1=int)),e(.),d(.),p(season+survey[int_p6])	1189.22	4.69	0.01	0.10	16
psi(.),gam(.),eps(prop_upland_3kmT(eps1=int)),e(.),d(.),p(season+survey[int_p6])	1189.24	4.71	0.01	0.09	16
psi(.),gam(.),eps(edge_mdwet_5kmT(eps1=int)),e(.),d(.),p(season+survey[int_p6])	1189.24	4.71	0.01	0.09	16
psi(.),gam(.),eps(prop_wet_540mQ(eps1=int)),e(.),d(.),p(season+survey[int_p6])	1189.32	4.79	0.01	0.09	17
psi(.),gam(.),eps(prop_upland_270m(eps1=int)),e(.),d(.),p(season+survey[int_p6])	1189.34	4.81	0.01	0.09	16
psi(.),gam(.),eps(prop_upland_3kmQ(eps1=int)),e(.),d(.),p(season+survey[int_p6])	1189.35	4.82	0.01	0.09	17
psi(.),gam(.),eps(prop_upland_270mT(eps1=int)),e(.),d(.),p(season+survey[int_p6])	1189.35	4.82	0.01	0.09	16
psi(.),gam(.),eps(prop_wet_540m(eps1=int)),e(.),d(.),p(season+survey[int_p6])	1189.48	4.95	0.01	0.08	16
psi(.),gam(.),eps(prop_upland_3km(eps1=int)),e(.),d(.),p(season+survey[int_p6])	1189.50	4.97	0.01	0.08	16
psi(.),gam(.),eps(count_conif_can(eps1=int)),e(.),d(.),p(season+survey[int_p6])	1189.50	4.97	0.01	0.08	16

psi(.),gam(.),eps(count_conif_canT(eps1=int)),e(.),d(.),p(season+survey[int_p6])	1189.76	5.23	0.01	0.07	16
psi(.),gam(.),eps(prop_upland_540m(eps1=int)),e(.),d(.),p(season+survey[int_p6])	1189.77	5.24	0.01	0.07	16
psi(.),gam(.),eps(prop_upland_540mT(eps1=int)),e(.),d(.),p(season+survey[int_p6])	1189.78	5.25	0.01	0.07	16
psi(.),gam(.),eps(prop_upland_1kmT(eps1=int)),e(.),d(.),p(season+survey[int_p6])	1189.9	5.37	0.01	0.07	16
psi(.),gam(.),eps(prop_upland_5kmQ(eps1=int)),e(.),d(.),p(season+survey[int_p6])	1189.93	5.40	0.01	0.07	17
psi(.),gam(.),eps(prop_wet_270m(eps1=int)),e(.),d(.),p(season+survey[int_p6])	1189.97	5.44	0.01	0.07	16
psi(.),gam(.),eps(prop_wet_270mT(eps1=int)),e(.),d(.),p(season+survey[int_p6])	1190.02	5.49	0.01	0.06	16
psi(.),gam(.),eps(prop_upland_1km(eps1=int)),e(.),d(.),p(season+survey[int_p6])	1190.06	5.53	0.01	0.06	16
psi(.),gam(.),eps(edge_mdwet_1kmQ(eps1=int)),e(.),d(.),p(season+survey[int_p6])	1190.10	5.57	0.01	0.06	17
psi(.),gam(.),eps(count_conif_canQ(eps1=int)),e(.),d(.),p(season+survey[int_p6])	1190.24	5.71	0.01	0.06	17
psi(.),gam(.),eps(prop_conif_540m(eps1=int)),e(.),d(.),p(season+survey[int_p6])	1190.25	5.72	0.01	0.06	16
psi(.),gam(.),eps(prop_conif_540mT(eps1=int)),e(.),d(.),p(season+survey[int_p6])	1190.30	5.77	0.01	0.06	16
psi(.),gam(.),eps(prop_wet_1kmQ(eps1=int)),e(.),d(.),p(season+survey[int_p6])	1190.31	5.78	0.01	0.06	17
psi(.),gam(.),eps(prop_conif_270mT(eps1=int)),e(.),d(.),p(season+survey[int_p6])	1190.50	5.97	< 0.01	0.05	16
psi(.),gam(.),eps(prop_conif_270m(eps1=int)),e(.),d(.),p(season+survey[int_p6])	1190.51	5.98	< 0.01	0.05	16
psi(.),gam(.),eps(edge_mdwet_270m(eps1=int)),e(.),d(.),p(season+survey[int_p6])	1190.51	5.98	< 0.01	0.05	16
psi(.),gam(.),eps(basal_conif_canT(eps1=int)),e(.),d(.),p(season+survey[int_p6])	1190.52	5.99	< 0.01	0.05	16
psi(.),gam(.),eps(edge_mdwet_270mT(eps1=int)),e(.),d(.),p(season+survey[int_p6])	1190.56	6.03	< 0.01	0.05	16
psi(.),gam(.),eps(basal_conif_can(eps1=int)),e(.),d(.),p(season+survey[int_p6])	1190.56	6.03	< 0.01	0.05	16
psi(.),gam(.),eps(prop_conif_5kmQ(eps1=int)),e(.),d(.),p(season+survey[int_p6])	1190.93	6.4	< 0.01	0.04	17
psi(.),gam(.),eps(edge_mdwet_5kmQ(eps1=int)),e(.),d(.),p(season+survey[int_p6])	1190.96	6.43	< 0.01	0.04	17
psi(.),gam(.),eps(basal_conif_canQ(eps1=int)),e(.),d(.),p(season+survey[int_p6])	1191.25	6.72	< 0.01	0.03	17
psi(.),gam(.),eps(prop_upland_270mQ(eps1=int)),e(.),d(.),p(season+survey[int_p6])	1191.33	6.80	< 0.01	0.03	17
psi(.),gam(.),eps(prop_upland_1kmQ(eps1=int)),e(.),d(.),p(season+survey[int_p6])	1191.44	6.91	< 0.01	0.03	17
psi(.),gam(.),eps(prop_upland_540mQ(eps1=int)),e(.),d(.),p(season+survey[int_p6])	1191.71	7.18	< 0.01	0.03	17
psi(.),gam(.),eps(prop_conif_540mQ(eps1=int)),e(.),d(.),p(season+survey[int_p6])	1191.88	7.35	< 0.01	0.03	17

psi(.),gam(.),eps(prop_wet_270mQ(eps1=int)),e(.),d(.),p(season+survey[int_p6])	1191.96	7.43	< 0.01	0.02	17
psi(.),gam(.),eps(edge_mdwet_270mQ(eps1=int)),e(.),d(.),p(season+survey[int_p6])	1192.25	7.72	< 0.01	0.02	17

Appendix 11: Strengths of support for multivariate models of extinction and colonization of *E. marcellus* while keeping the best detection model constant. Psi = occupancy, p = detection, gam = colonization, eps = extinction, e = entry, and d = departure, full_id = season*survey interaction, rain = days since rain, Q = quadratic function ($x + x^2$), T = a pseudo-threshold function ($\ln[x]$), prop_paw = proportion meter intervals intercepted by *A. triloba*, edge_forwet = density of edges between forest and wetland, lidar = structural heterogeneity of vegetation 0.3-3.0 m above ground, edge_foroh = edge density forest open herbaceous, prop_ag = proportion of agriculture, and AIC = Akaike's Information Criterion adjusted for sample size, ΔAIC = difference from the top model AIC, and $AIC\omega$ = model weight.

Model	AIC	ΔAIC	$AIC\omega$	Model Likelihood	Number of parameters
psi(prop_pawpaw),gam(edge_foroh_3kmQ+prop_ag_270m),eps(edge_forwet_5km),e(.),d(.),p(full_id+rain)	1061.82	0.00	0.36	1.00	39
psi(prop_pawpaw),gam(edge_foroh_3kmQ+prop_ag_270m),eps(lidar+edge_forwet_5km),e(.),d(.),p(full_id+rain)	1063.19	1.37	0.18	0.50	40
psi(prop_pawpaw),gam(edge_foroh_3kmQ),eps(edge_forwet_5km),e(.),d(.),p(full_id+rain)	1063.26	1.44	0.18	0.49	38
psi(prop_pawpaw),gam(edge_foroh_3kmQ),eps(lidar+edge_forwet_5km),e(.),d(.),p(full_id+rain)	1064.56	2.74	0.09	0.25	39
psi(prop_pawpaw),gam(edge_foroh_3kmQ+prop_ag_270m),eps(lidar),e(.),d(.),p(full_id+rain)	1064.70	2.88	0.09	0.24	39
psi(prop_pawpaw),gam(edge_foroh_3kmQ),eps(lidar),e(.),d(.),p(full_id+rain)	1065.69	3.87	0.05	0.14	38
psi(prop_pawpaw),gam(full_id),eps(edge_forwet_5km),e(.),d(.),p(full_id+rain)	1067.97	6.15	0.02	0.05	36
psi(prop_pawpaw),gam(full_id),eps(lidar+edge_forwet_5km),e(.),d(.),p(full_id+rain)	1069.06	7.24	0.01	0.03	37
psi(prop_pawpaw),gam(edge_foroh_3kmQ+prop_ag_270m),eps(full_id),e(.),d(.),p(full_id+rain)	1070.10	8.28	0.01	0.02	38
psi(prop_pawpaw),gam(full_id),eps(lidar),e(.),d(.),p(full_id+rain)	1070.13	8.31	0.01	0.02	36
psi(prop_pawpaw),gam(edge_foroh_3kmQ),eps(full_id),e(.),d(.),p(full_id+rain)	1070.85	9.03	<0.01	0.01	37
psi(prop_pawpaw),gam(prop_ag_270m),eps(full_id),e(.),d(.),p(full_id+rain)	1072.70	10.88	<0.01	<0.01	36

psi(.),gam(edge_foroh_3kmQ+prop_ag_270m),eps(edge_forwet_5km),e(.),d(.),p(full_id+rain)	1073.16	11.34	<0.01	<0.01	38
psi(.),gam(edge_foroh_3kmQ+prop_ag_270m),eps(lidar+edge_forwet_5km),e(.),d(.),p(full_id+rain)	1074.53	12.71	<0.01	<0.01	39
psi(.),gam(.),eps(.),e(.),d(.),p(full_id+rain)	1081.92	20.10	<0.01	<0.01	30
psi(.),gam(full_id),eps(full_id),e(.),d(.),p(full_id+rain)	1087.71	25.89	<0.01	<0.01	34

Appendix 12: Strengths of support for multivariate models of colonization and extinction of *P. glaucus* while keeping the best detection model constant. Psi = occupancy, p = detection, gam = colonization, eps = extinction, e = entry, and d = departure, survey[int_p6] = survey 6 set as intercept, Q = quadratic function ($x + x^2$), T = a pseudo-threshold function ($\ln[x]$), host_us = count host understory, oh = proportion open herbaceous, forwet = edge density forest-wet, wet = proportion wetland, mdwet = mixed/decid forest-wetland, local = road local, conif = proportion coniferous, and AIC = Akaike's Information Criterion adjusted for sample size, ΔAIC = difference from the top model AIC, LL = log-likelihood, and $AIC\omega$ = model weight.

Model	AIC	ΔAIC	$AIC\omega$	Model Likelihood	Number of parameters
psi(host_us),gam(m1_oh3km),eps(m1_forwet540m),e(.),d(.),p(season+survey[int_p6])	1173.65	0.00	0.26	1.00	19
psi(host_us),gam(m1_oh3km),eps(m2_forwet540m),e(.),d(.),p(season+survey[int_p6])	1174.61	0.96	0.16	0.62	20
psi(host_us),gam(m1_oh3km),eps(m1_wet3km),e(.),d(.),p(season+survey[int_p6])	1175.34	1.69	0.11	0.43	19
psi(host_us),gam(m1_local3km),eps(m2_forwet540m),e(.),d(.),p(season+survey[int_p6])	1175.69	2.04	0.09	0.36	20
psi(host_us),gam(m1_local3km),eps(m1_wet3km),e(.),d(.),p(season+survey[int_p6])	1176.10	2.45	0.08	0.29	19
psi(host_us),gam(m1_oh3km),eps(m1_mdwet3km),e(.),d(.),p(season+survey[int_p6])	1176.36	2.71	0.06	0.26	19
psi(host_us),gam(m1_oh3km),eps(m1_conif1km),e(.),d(.),p(season+survey[int_p6])	1176.64	2.99	0.06	0.22	19
psi(host_us),gam(m1_local3km),eps(m1_mdwet3km),e(.),d(.),p(season+survey[int_p6])	1177.2	3.55	0.04	0.17	19
psi(host_us),gam(m1_local3km),eps(m1_conif1km),e(.),d(.),p(season+survey[int_p6])	1177.65	4.00	0.03	0.14	19
psi(host_us),gam(m1_oh3km),eps(m1_wet3km+conif1km),e(.),d(.),p(season+survey[int_p6])	1177.68	4.03	0.03	0.13	20
psi(host_us),gam(m1_oh3km),eps(m1_mdwet3km+conif1km),e(.),d(.),p(season+survey[int_p6])	1178.07	4.42	0.03	0.11	20
psi(host_us),gam(m1_local3km),eps(m1_wet2km+conif1km),e(.),d(.),p(season+survey[int_p6])	1178.58	4.93	0.02	0.09	20
psi(host_us),gam(m1_local3km),eps(m1_mdwet3km+conif1km),e(.),d(.),p(season+survey[int_p6])	1178.94	5.29	0.01	0.07	20
psi(.),gam(.),eps(.),e(.),d(.),p(season+survey[int_p6])	1188.77	15.12	<0.01	<0.01	14